Determining the strong coupling: status and challenges

Antonio Pich

IFIC, Universitat de València – CSIC, Apt. Correus 22085, E-46071 València, Spain.
E-mail: pich@ific.uv.es

Juan Rojo

Department of Physics and Astronomy, VU University, De Boelelaan 1081, 1081 HV Amsterdam,
and Nikhef Theory Group, Science Park 105, 1098 XG Amsterdam, The Netherlands.
E-mail: j.rojo@vu.nl

Rainer Sommer

John von Neumann Institute for Computing (NIC), DESY, Platanenallee 6, D-15738 Zeuthen,
Germany.
E-mail: rainer.sommer@desy.de

Antonio Vairo

Physik-Department, Technische Universität München, James-Franck-Str. 1, 85748 Garching,
Germany.
E-mail: antonio.vairo@tum.de

The "XIIIth Quark Confinement and the Hadron Spectrum" conference (Confinement 2018) contained a "Round Table Discussion" on the status of the determinations of the strong coupling $\alpha_s(m_Z)$ as well as prospects for future improvements. In this contribution, we summarize the different aspects of the discussion. In particular, we cover α_s determinations from inclusive observables, such as the hadronic decays of the Z boson and the τ lepton; from global fits of parton distribution functions (PDFs); from high-energy collider observables, and from event shapes; as well as from various observables computed by lattice QCD, specifically from the QCD static energy. There is overall good agreement between these various determinations, but there are also outliers, differing from the world average by up to -5%. Nevertheless, the general agreement constitutes a beautiful and significant test of the detailed nature of the strong interactions, and provides a crucial input for high-precision calculations in QCD and beyond.

1. Introduction

Quantum Chromodynamics (QCD) contains only a single free parameter, the value of its coupling constant, besides the values of the quark masses. Therefore, all strong interaction phenomena should be described in terms of the unique strong coupling α_s. The overwhelming consistency of the many determinations of α_s, performed in very different processes and in a broad range of energy scales, provides a beautiful verification of QCD, establishing the SU(3)$_C$ gauge theory as the fundamental quantum field theory of the strong interaction.

The impressive progress achieved in recent years has promoted perturbative QCD to the status of precision physics, improving in a very sizeable way the physics potential of the current LHC program. In the $\overline{\text{MS}}$-scheme the QCD β function is known to five loops [1, 2, 3, 4], which provides a precise theoretical control of the renormalization-scale dependence of the running coupling. Moreover, the very modest growth of the β-function coefficients with the perturbative order gives rise to a surprisingly smooth power expansion. The β function and, therefore, the running coupling depend on the number of active quark flavours n_f. The matching conditions relating the effective QCD theories with n_f and $n_f - 1$ quark flavours are known to four loops [5, 6].

At the current level of accuracy, a very good understanding of the uncertainties associated with the different measurements of α_s is needed. Thus, we should restrict the analysis to observables where perturbative techniques are reliable and enough terms in the expansion in powers of α_s are available. Following the Particle Data Group (PDG) criteria [7], in this contribution we will require a NNLO or higher accuracy. Non-perturbative contributions and theoretical uncertainties from the expected asymptotic behaviour of perturbation theory should also be under good control.

The outline of this contribution is the following. First of all, in Sect. 2, we review the determinations of α_s from inclusive observables such as the hadronic τ decay width and the $Z \rightarrow$ hadrons branching fraction. Then, in Sect. 3, we discuss determinations from global PDF fits, high-energy collider observables, and event shapes. In Sect. 4, we study extractions of the strong coupling from the lattice QCD static energy. Then in Sect 5, we review recent progress in determining $\alpha_s(m_Z)$ from lattice QCD calculations more generally. Finally in Sect. 6 we present some general reflections about the main lessons that can be drawn from this discussion exercise.

2. Inclusive observables *(A. Pich)*

The inclusive electroweak production of hadrons provides clean observables that can be accurately predicted with perturbative tools, such as the cross section $\sigma(e^+e^- \rightarrow \text{hadrons})$ or the decay widths $\Gamma(Z \rightarrow \text{hadrons})$ and $\Gamma(W \rightarrow \text{hadrons})$. The final hadrons are produced through the colour-singlet vector $V_{ij}^\mu = \bar{\psi}_j \gamma^\mu \psi_i$ and axial-vector $A_{ij}^\mu = \bar{\psi}_j \gamma^\mu \gamma_5 \psi_i$ quark currents ($i, j = u, d, s \ldots$). The QCD dynamics is governed by the corresponding two-point correlation functions ($J = V, A$)

$$\Pi_{ij,J}^{\mu\nu}(q) \equiv i \int d^4x\, e^{iqx} \langle 0|T(J_{ij}^\mu(x) J_{ij}^\nu(0)^\dagger)|0\rangle = \left(-g^{\mu\nu}q^2 + q^\mu q^\nu\right) \Pi_{ij,J}^{(0+1)}(q^2) + g^{\mu\nu}q^2 \Pi_{ij,J}^{(0)}(q^2).$$

(2.1)

The scalar functions $\Pi_{ij,J}^{(L)}(q^2)$ (the superscript $L = 0, 1$ denotes the angular momentum in the hadronic rest frame) are analytic in the whole complex q^2 plane, except along the (physical) positive real axis where their imaginary parts have discontinuities. These absorptive cuts correspond to the measurable hadronic spectral distributions with the given quantum numbers.

For massless quarks, $\Pi_{ij,V}^{(0)}(s) = 0$ while $s\Pi_{ij,A}^{(0)}(s)$ is a known constant generated by the non-perturbative Goldstone-pole contribution that cancels in $\Pi_{ij,A}^{(0+1)}(s)$. When $i \neq j$, the two quark currents must necessarily be connected through a quark loop (non-singlet topology), which gives identical contributions to the vector and axial massless correlators: $\Pi_{i\neq j,V}^{(0+1)}(s) = \Pi_{i\neq j,A}^{(0+1)}(s)$. The neutral-current correlators ($i = j$) get additional singlet contributions, where each current couples to a different quark loop. Since gluons have $J^{PC} = 1^{--}$ and colour, these singlet topologies start to contribute at $\mathcal{O}(\alpha_s^3)$ and $\mathcal{O}(\alpha_s^2)$, respectively, for the vector and axial-vector currents.

The perturbative expansion of the correlators $\Pi_{ij,J}^{(0+1)}(s)$ is known with an impressive $\mathcal{O}(\alpha_s^4)$ accuracy [8, 9, 10]. Therefore, the ratio $R_{e^+e^-}(s) \equiv \sigma(e^+e^- \to \text{hadrons})/\sigma(e^+e^- \to \mu^+\mu^-)$, which is proportional to the imaginary part of the electromagnetic vector-current correlator, could be used to perform a clean N^{3}LO determination of α_s, at energies high enough to safely neglect non-perturbative contributions. The experimental uncertainties are, however, too large to get a competitive value.

$\Gamma(Z \to \text{hadrons})$. The electroweak neutral quark current contains vector and axial-vector components, weighted with the corresponding Z couplings. The large value of the top mass generates sizeable singlet axial corrections which start at $\mathcal{O}(\alpha_s^2)$. The ratio of the hadronic and electronic widths of the Z boson is given by the perturbative QCD series ($m_b = 0$, $m_t \neq 0$, $n_f = 5$)

$$R_Z \equiv \frac{\Gamma(Z \to \text{hadrons})}{\Gamma(Z \to e^+e^-)} = R_Z^{\text{EW}} N_C \left\{ 1 + \sum_{n=1} \tilde{F}_n \left(\frac{\alpha_s(m_Z)}{\pi} \right)^n \right\}, \qquad (2.2)$$

with $\tilde{F}_1 = 1$, $\tilde{F}_2 = 0.76264$, $\tilde{F}_3 = -15.490$ and $\tilde{F}_4 = -68.241$ [9]. Taking into account electroweak corrections and QCD contributions suppressed by powers of m_b^2/m_Z^2 [11, 12], the ratio R_Z is included in the global fit to electroweak precision data. One obtains in this way a quite accurate value of $\alpha_s(m_Z)$ [13]:

$$\alpha_s^{(n_f=5)}(m_Z) = 0.1196 \pm 0.0030. \qquad (2.3)$$

Since this result assumes the validity of the electroweak Standard Model, its comparison with other determinations of the strong coupling provides a non-trivial constraint on new-physics scenarios.

$\Gamma(\tau \to \nu_\tau + \text{hadrons})$. The current precision on the hadronic decay width of the $W^\pm$ boson is not good enough to perform an accurate determination of α_s. A much more sensitive observable is the hadronic τ decay width [14, 15, 16, 17], which proceeds through a virtual $W^\pm$ boson. Restricting the analysis to the dominant Cabibbo-allowed decay width,

$$R_{\tau,V+A} \equiv \frac{\Gamma[\tau^- \to \nu_\tau + \text{hadrons}\,(S=0)]}{\Gamma[\tau^- \to \nu_\tau e^- \bar{\nu}_e]} \qquad (2.4)$$

$$= 12\pi |V_{ud}|^2 S_{\text{EW}} \int_0^{m_\tau^2} \frac{ds}{m_\tau^2} \left(1 - \frac{s}{m_\tau^2} \right)^2 \left[\left(1 + 2\frac{s}{m_\tau^2} \right) \text{Im}\Pi_{ud,V+A}^{(0+1)}(s) - 2\frac{s}{m_\tau^2} \text{Im}\Pi_{ud,V+A}^{(0)}(s) \right],$$

where $S_{\text{EW}} = 1.0201 \pm 0.0003$ incorporates the electroweak radiative corrections [18, 19, 20]. The measured invariant-mass distribution of the final hadrons determines the spectral functions $\rho_J(s) \equiv \text{Im}\Pi_{ud,J}^{(0+1)}(s)/\pi$, shown in figure 1 (the only relevant contribution to the $s\,\text{Im}\Pi_{ud,V+A}^{(0)}(s)$ term is the π^- final state at $s = m_\pi^2$).
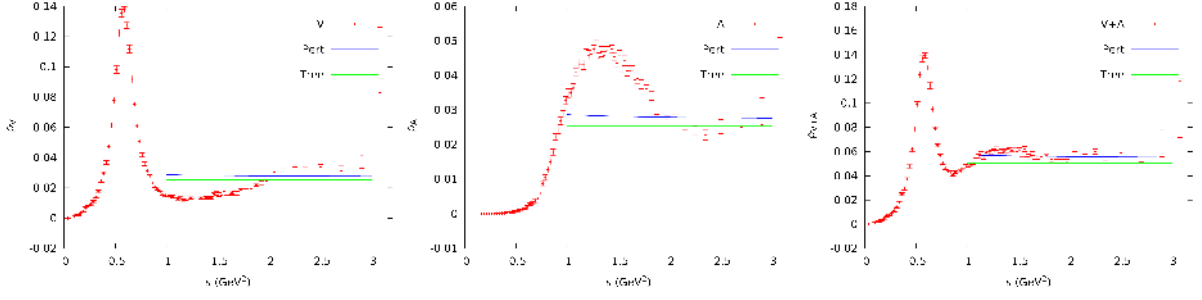
Figure 1: Spectral functions for the V, A and $V + A$ channels, determined from ALEPH τ data [21].

Although the low-energy spectral functions themselves cannot be described with perturbative tools, the analyticity properties of the $\Pi_{ij,J}^{(L)}(s)$ correlators relate weighted integrals (moments) of the experimental spectral distribution with theoretical QCD predictions [17, 22]:

$$A_J^{\omega}(s_0) \equiv \int_{s_{\text{th}}}^{s_0} \frac{ds}{s_0} \, \omega(s) \, \text{Im}\Pi_{ud,J}^{(0+1)}(s) \;=\; \frac{i}{2} \oint_{|s|=s_0} \frac{ds}{s_0} \, \omega(s) \, \Pi_{ud,J}^{(0+1)}(s). \tag{2.5}$$

The complex integral in the right-hand side (rhs) runs counter-clockwise around the circle $|s| = s_0$, s_{th} is the hadronic mass-squared threshold and $\omega(s)$ is any weight function analytic in $|s| \le s_0$. While the left-hand-side integral is directly determined by the experimental data, for large-enough values of s_0 the operator product expansion (OPE), $\Pi_{ud,J}^{(0+1)}(s)^{\text{OPE}} = \sum_D \mathcal{O}_{D,J}/(-s)^{D/2}$, can be used to predict the contour integral as an expansion in inverse powers of s_0, the perturbative contribution being the leading $D = 0$ term. Contributions to the rhs integral from the region near the real axis, where the OPE is not valid, can be efficiently suppressed with 'pinched' weights that vanish at $s = s_0$.

The ratio $R_{\tau,V+A}$ involves the doubly-pinched weight $\omega(x) = (1-x^2)(1+2x) = 1 - 3x^2 + 2x^3$, with $x \equiv s/s_0$ and $s_0 = m_\tau^2$. Cauchy's theorem implies that the contour integral is only sensitive to OPE corrections with $D = 6$ and 8, which are strongly suppressed by the corresponding powers of the τ mass. In addition, the $D = 6$ vector and axial-vector contributions have opposite signs, cancelling to a large extent. Therefore, $R_{\tau,V+A}$ is a clean observable to determine α_s. It is known with $\mathcal{O}(\alpha_s^4)$ precision, and it is very sensitive to the strong coupling because $\alpha_s(m_\tau)$ is sizeable. The small non-perturbative corrections can be directly estimated from the data, using weights with the appropriate power of s to project a particular OPE contribution [22]. The dominant theoretical uncertainty is the perturbative error associated with the unknown higher-order corrections. For a given value of α_s, a truncated fixed-order perturbation theory (FOPT) approximation [17] leads to a larger perturbative contribution than the so-called contour-improved perturbation theory (CIPT) [23, 24], which resums large corrections arising from the long running of the strong coupling along the circle $s = s_0$. Therefore, FOPT results in a smaller fitted value of $\alpha_s(m_\tau)$ than CIPT.

The predicted suppression of non-perturbative corrections [17] has been confirmed through detailed analyses of the invariant-mass distribution of the hadronic τ decay products, performed by ALEPH [25, 26, 27, 28, 29], CLEO [30] and OPAL [31], showing that these effects are below 1% in $R_{\tau,V+A}$. In comparison, the purely perturbative contribution is around 20%. The most complete and precise experimental study, performed with the recently updated ALEPH data, gives $\alpha_s^{(n_f=3)}(m_\tau) =$

3

Method	$\alpha_s^{(n_f=3)}(m_\tau)$		
	CIPT	FOPT	Average
ALEPH moments	$0.339^{+0.019}_{-0.017}$	$0.319^{+0.017}_{-0.015}$	$0.329^{+0.020}_{-0.018}$
Modified ALEPH moments	$0.338^{+0.014}_{-0.012}$	$0.319^{+0.013}_{-0.010}$	$0.329^{+0.016}_{-0.014}$
$A^{(2,m)}$ moments	$0.336^{+0.018}_{-0.016}$	$0.317^{+0.015}_{-0.013}$	$0.326^{+0.018}_{-0.016}$
s_0 dependence	0.335 ± 0.014	0.323 ± 0.012	0.329 ± 0.013
Borel transform	$0.328^{+0.014}_{-0.013}$	$0.318^{+0.015}_{-0.012}$	$0.323^{+0.015}_{-0.013}$
Average	0.335 ± 0.013	0.320 ± 0.012	0.328 ± 0.013

Table 1: Determinations of $\alpha_s^{(n_f=3)}(m_\tau)$ from τ decay data, in the $V+A$ channel [38].

$0.332 \pm 0.005_{\mathrm{exp}} \pm 0.011_{\mathrm{th}}$ [21], where the second error takes into account the different central values obtained with the FOPT (0.324) and CIPT (0.341) prescriptions. Taking as input the small non-perturbative contribution extracted from the ALEPH analysis, the strong coupling can also be determined from the total τ hadronic width (and/or lifetime); this gives $\alpha_s^{(n_f=3)}(m_\tau) = 0.331 \pm 0.013$ (FOPT + CIPT) [32], in perfect agreement with the ALEPH result.

Slightly smaller (10%) values of $\alpha_s(m_\tau)$ have been obtained in Ref. [33] through a direct fit of the vector spectral function from $s = \hat{s}_0 = 1.55\,\mathrm{GeV}^2$ to m_τ^2, with a 4-parameter ansatz for $\rho_V(s)$, plus the moment $A_V^{\omega=1}(\hat{s}_0)$. This approach maximizes the role of non-perturbative effects in order to better study them [34, 35], but this is not a good strategy to perform an accurate determination of the strong coupling. The OPE is actually not valid on the physical cut and the quoted uncertainties are largely underestimated [36, 37]. A more careful numerical study has shown that the fitted results strongly depend on the chosen value of $\hat{s}_0$ and the particular form of the assumed spectral-function ansatz [38]: fluctuations of $\alpha_s(m_\tau)$ larger than 3σ are obtained with slight modifications of these assumptions, showing that the fitted value is model dependent.

Ref. [38] has performed an exhaustive reanalysis of the τ determination of the strong coupling, including many consistency checks to assess the actual size of non-perturbative effects. All strategies adopted in previous works and several complementary approaches have been investigated, studying the stability of the results and trying to uncover any potential hidden weaknesses. Once their uncertainties are properly estimated, all adopted methodologies result in very consistent values of $\alpha_s(m_\tau)$. Table 1 summarizes the most reliable and precise determinations. The first three lines show the results obtained with different types of (at least doubly-pinched) weights, which are sensitive to different power corrections. The amazing stability of the fitted values reflects the very minor numerical effect of OPE corrections, which has been confirmed through many other additional tests. The fourth line extracts the information from the s_0 dependence of a single moment with $\omega^{(2,m)}(x) = 1 - (m+2)x^{m+1} + (m+1)x^{m+2}$, for $m = 0, 1, 2$; although this is much more sensitive to potential violations of quark-hadron duality, it results in values of the strong coupling fully compatible with the determinations in the first three lines. The fifth line adopts weights of the form $(1 - x^{m+1})e^{-ax}$ that suppress violations of duality, but paying the price of a potentially larger sensitivity to power corrections.

The overall agreement of all determinations in Table 1 shows their robustness and reliability.

As expected, there is a systematic difference between CIPT and FOPT; the last column averages the results from both prescriptions, but adding in quadrature half their difference as an additional systematic error. Averaging the five determinations, but keeping the smaller uncertainties to account for the large correlations, one finds the values indicated in the last line. From the average of the five combined (CIPT and FOPT) results in the last column, one finally gets

$$\alpha_s^{(n_f=3)}(m_\tau) = 0.328 \pm 0.013, \tag{2.6}$$

in very good agreement with the ALEPH determination of the strong coupling mentioned before.

After evolution up to the scale m_Z, the value of $\alpha_s^{(n_f=3)}(m_\tau)$ in (2.6) decreases to

$$\alpha_s^{(n_f=5)}(m_Z) = 0.1197 \pm 0.0015, \tag{2.7}$$

which nicely agrees with the direct measurement at the Z peak in Eq. (2.3). The comparison of these two determinations provides a beautiful test of the predicted QCD running; i.e., a very significant experimental verification of asymptotic freedom:

$$\alpha_s^{(n_f=5)}(m_Z)\Big|_\tau - \alpha_s^{(n_f=5)}(m_Z)\Big|_Z = 0.0001 \pm 0.0015_\tau \pm 0.0030_Z . \tag{2.8}$$

Notice the order-of-magnitude difference between the errors in (2.6) and (2.7), which exhibits the much higher sensitivity to the strong coupling at lower energies.

High-precision measurements of the spectral functions, especially in the higher kinematically-allowed energy bins, would be required in order to improve the α_s determination from τ decay. Both higher statistics and a good control of experimental systematic uncertainties are needed, which could be possible at the Belle-II experiment. An improved understanding of higher-order perturbative corrections is also needed. While τ decay data are kinematically limited to $s \leq m_\tau^2$, higher values of the hadronic invariant mass can be accessed in e^+e^- annihilation. However, in the vector spectral function the onset of the QCD asymptotic behaviour is unfortunately also reached at larger values of s, as exhibited in Fig. 1 for its $I = 1$ component. The more inclusive nature of the $V + A$ channel leads to a much flatter distribution, which is related with the smaller non-perturbative corrections to the spectral moments. Nevertheless, e^+e^- data provide useful complementary information that can be analysed through spectral moments in the same way than with τ decay data [39, 40]. The integrated distributions provide in fact a better sensitivity to α_s than the ratio $R_{e^+e^-}(s)$. However, owing to the current experimental precision, the resulting uncertainty on α_s is larger than the one achieved with τ data [41].

3. Global PDF fits and collider measurements   *(J. Rojo)*

The determination of the strong coupling constant from fits of parton distribution functions (PDFs) has a long history. In a joint determination of PDFs and $\alpha_s(m_Z)$, the sensitivity to the latter arises from two different aspects of the fit. On the one hand, through the scaling violations induced by DGLAP evolution, which are particularly strong at small x. On the other hand, from the partonic matrix elements for those input processes that are driven by QCD scattering already at the Born level, such as jet production. In this context, modern PDF fits (see [42, 43, 44] for recent reviews) contain a wide variety of hadron collider data sensitive to the value of the strong coupling,
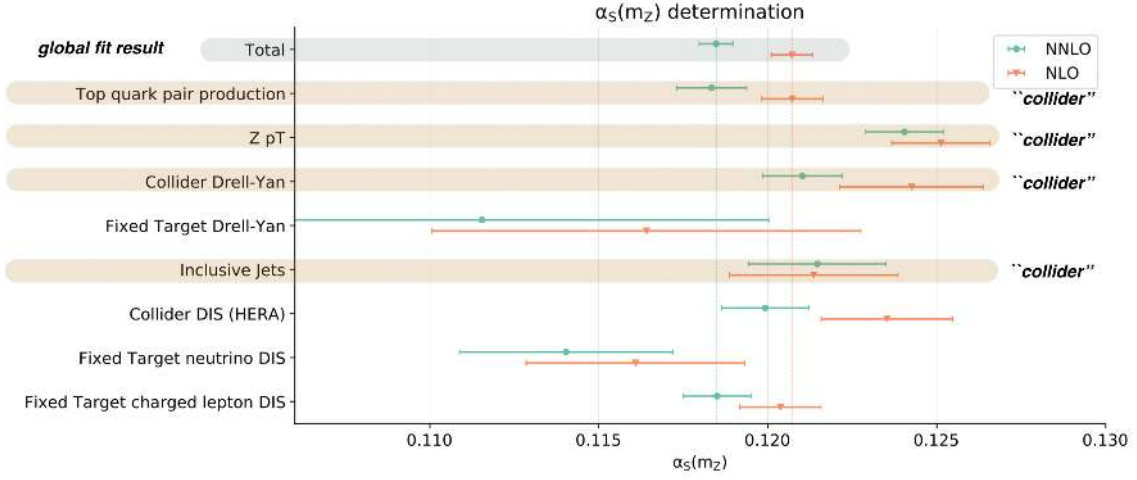
Figure 2: Modern PDF fits contain a wide variety of hadron collider data sensitive to the value of the strong coupling. Here we compare the values of $\alpha_s(m_Z)$ obtained in the NNPDF3.1 NLO and NNLO global fits with those obtained from the reduced χ^2 restricted to specific families of processes. Several of them, such as inclusive jets and top quark production, are often used as input for independent determinations of $\alpha_s(m_Z)$.

from inclusive jets [45] to direct photon [46], the transverse momentum of Z bosons [47] and top quark pair production [48], and therefore offer unique opportunities for precision determinations of $\alpha_s(m_Z)$. In addition, several of these processes such as inclusive jets and top quark production are often used as input for independent determinations of $\alpha_s(m_Z)$. Here we first review selected recent determinations of $\alpha_s(m_Z)$ in the context of global PDF fits, and then those determinations based on collider measurements that do not involve a simultaneous PDF extraction.

Determinations within PDF fits. The most recent determination of $\alpha_s(m_Z)$ from a global PDF fit is [49] based on the NNPDF3.1 analysis [50]. This study finds that at NNLO one has

$$\alpha_s(m_Z) \equiv \alpha_s^{(n_f=5)}(m_Z) = 0.1185 \pm 0.0005_{\text{exp}} \pm 0.0011_{\text{th}}, \tag{3.1}$$

where the theory error from missing higher-order (MHO) corrections at $\mathcal{O}\left(\alpha_s^3\right)$ is conservatively estimated from the half-shift between NLO and NNLO. This global analysis is based on a comprehensive set of input data from the precise HERA structure functions to jet, electroweak gauge boson, and top quark production at the Tevatron and the LHC. Crucially, many of these processes exhibit a direct (and complementary) sensitivity to α_s. Theoretical calculations are based on exact NNLO QCD fixed-order theory, which for most processes used in the fit have become available only very recently.

In Fig. 2 we compare the values of $\alpha_s(m_Z)$ obtained in the NNPDF3.1 NLO and NNLO global fits with those obtained from the "reduced" χ^2 restricted to specific families of processes, which we define by keeping all PDFs fixed to their best-fit values in the global analysis, while examining now how the χ^2 contribution of a specific family varies with the value of the strong coupling α_s. From this study, one then finds that the value of $\alpha_s(m_Z)$ appears to be determined from the combination of several classes of process that carry a similar weight in terms of their sensitivity to the strong coupling: $t\bar{t}$ production, Z p_T, collider gauge boson production, and collider and fixed-target deep-
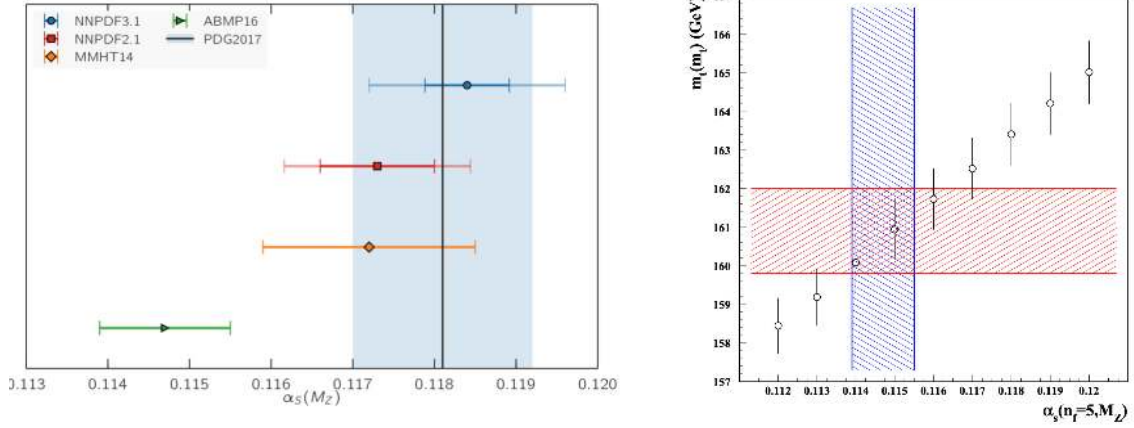
Figure 3: Left: comparison of the $\alpha_s(m_Z)$ values determined in the NNPDF3.1, NNPDF2.1, MMHT14, and ABMP16 PDF fits compared to the PDG17 average. Right: the correlation between the fitted values of $\alpha_s(m_Z)$ and $m_t(m_t)$ obtained in the ABMP16 analysis; figure reproduced from [54].

inelastic scattering. In other words, there is not a single process that dominates the extraction of α_s from the global PDF, but rather the interplay between many of them with comparable weight.

In Fig. 3 (left) we compare the $\alpha_s(m_Z)$ values determined in the NNPDF3.1, NNPDF2.1 [51, 52], MMHT14 [53], and ABMP16 [54] PDF fits with the current PDG average [7], namely

$$\alpha_s^{(\text{pdg})}(m_Z) = 0.1181 \pm 0.0011 . \tag{3.2}$$

For the NNPDF results, the inner error band includes the experimental and procedural uncertainties while the outer bar includes as well the theoretical MHO uncertainties. Both the NNPDF and the MMHT14 results agree within them as well as with the PDG averages. On the other hand, the ABMP16 determination is markedly lower. These differences can be partly explained by differences in the input dataset as well as in the treatment of heavy quark mass effects in the deep-inelastic structure functions, as discussed in [55, 56]. From the NNPDF3.1 result in Fig. 3 we can also see that, provided MHO uncertainties can be robustly estimated and reduced to a level comparable or below the experimental uncertainties, the determination of $\alpha_s(m_Z)$ from the global fit could become one of the dominant ingredients in the PDG average.

In a similar way that MHO uncertainties affect the $\alpha_s(m_Z)$ determination from the global fit (even though they are often neglected), one needs to account for the effects of other theory uncertainties such as the input values of the heavy quark masses. For example, in the description of top quark pair production cross sections, changes in the PDFs and α_s can be partially compensated by changes in the top quark mass m_t. This is illustrated in the right panel of Fig. 3, which shows the correlation between the fitted values of $\alpha_s(m_Z)$ and $m_t(m_t)$ obtained in the ABMP16 analysis. As discussed in [48], the dependence on the value of m_t can be efficiently suppressed by fitting normalised differential distributions where the dependence on the top quark mass cancels out.

Determinations from individual collider measurements. The same sensitivity to the value of $\alpha_s(m_Z)$ that specific collider measurements provide within the global PDF fit (see Fig. 2) can also be exploited to provide independent determinations that do not involve the simultaneous extraction
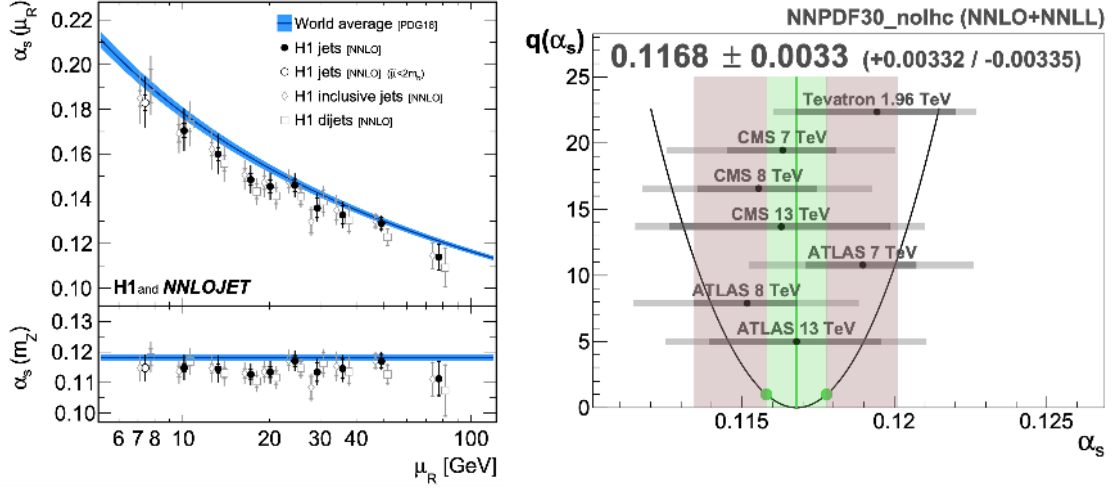
7

Figure 4: Left: summary of determinations of α_s from jet production in DIS by the H1 experiment [60] based on NNLO QCD theory. We show results for both $\alpha_s(\mu_R)$ and $\alpha_s(m_Z)$, where μ_R indicates the typical scale of the process. Right: results of the determination of $\alpha_s(m_Z)$ from the total $t\bar{t}$ cross section reported in [63] using NNPDF3.0 noLHC as input PDF set.

of the PDFs, but that rather assume PDFs and their uncertainties as an external input, see *e.g.* [45] and references therein for the specific case of jet production. In this context, the recent availability of the NNLO QCD corrections for fully differential distributions in inclusive jet [57], dijet [58], and top quark pair production [59] has made possible a significant reduction of the MHO uncertainties associated to these collider determinations, which before were limited to NLO QCD accuracy.

To illustrate this point, recently the strong coupling was determined from jet production measurements (both inclusive jets and dijets) in deep-inelastic lepton-proton scattering by the H1 collaboration [60] using the recently available NNLO QCD calculation [61]. Two different determinations are presented in this study: one where PDFs and their uncertainties are taken as external input from previous determinations and another where $\alpha_s(m_Z)$ is fitted simultaneously with the PDFs based on the `xFitter` tool [62]. This analysis finds $\alpha_s(m_Z) = 0.1157 \pm 0.0020$ (exp) $\pm$ 0.0029 (th) and $\alpha_s(m_Z) = 0.1157 \pm 0.0028$ (tot) in each of the two cases. Therefore despite the use of NNLO QCD calculations, theory errors from MHOs are still significant. In the left panel of Fig. 4 we present a summary of the different H1 determinations of α_s from jet data using NNLO QCD theory. We show results for both $\alpha_s(\mu_R)$ and $\alpha_s(m_Z)$, where μ_R indicates the typical scale of the process.

As proposed for the first time in [64], the total cross section for top quark pair production at the LHC also provides a clean observable to determine the strong coupling. This sensitivity has been exploited in [63] to carry out an updated extraction of $\alpha_s(m_Z)$ from $\sigma(t\bar{t})$ based on data from the Tevatron Run II and the LHC 7, 8, and 13 TeV. In the right panel of Fig. 4 we show the results of this analysis using NNPDF3.0 noLHC [65] as input PDF set. The green line and band indicate the central value of the combination of all collider measurements and the associated one-sigma experimental uncertainty, while the red band includes as well the MHO, PDF, and m_t theoretical uncertainties. Their final combined result is $\alpha_s(m_Z) = 0.1177 \pm 0.0035$, in agreement with the PDG average.
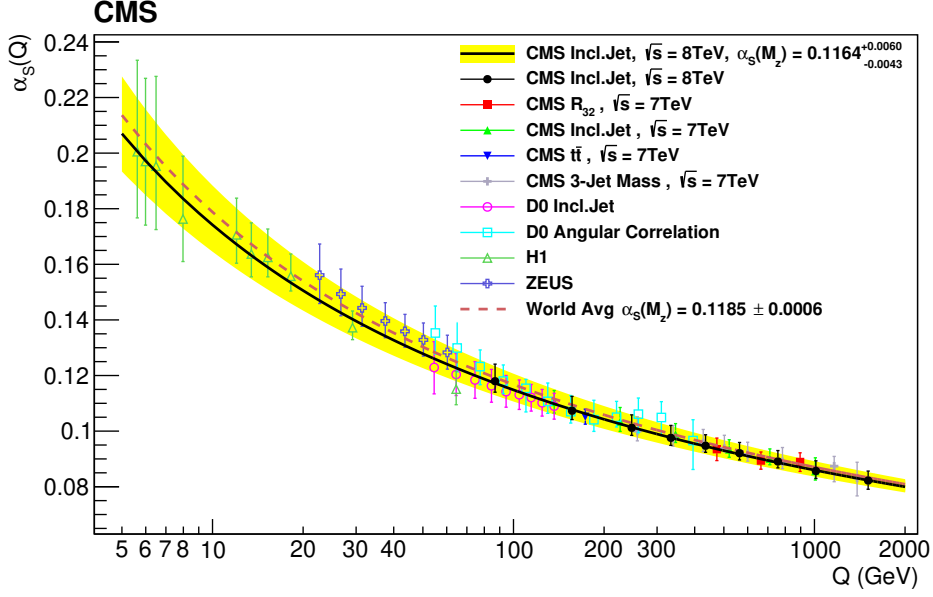
Figure 5: Summary of recent determinations of $\alpha_s(m_Z)$ at the LHC from the CMS experiment, compared to previous results by the Tevatron and HERA as well as with the global PDG average. Results are presented as a function of Q, the characteristic energy scale involved in each specific determination.

Other related determinations of $\alpha_s(m_Z)$ from collider cross sections, which do not involve simultaneously PDF extractions, are the CMS determination based on the $R_{3/2}$ ratio of three-to-two jet cross sections [66] and on the inclusive jet cross section [67] at 7 TeV and the ATLAS determinations based on the transverse energy-energy correlation [68] and the dijet azimuthal correlation [69] in jet production at 8 TeV.

To provide a general overview, in Fig. 5 we show a summary of recent determinations of $\alpha_s(m_Z)$ at the LHC from the CMS experiment, compared to previous results by the Tevatron and HERA as well as with the global PDG average. Results are presented as a function of Q, the typical energy scale involved in each specific determination. We can see how only the LHC determinations have a direct coverage of the TeV region, which is also important in searches of new heavy particles as we discuss next.

Testing the running of $\alpha_s(Q)$ in the TeV scale. In addition to the precision determination of the strong coupling at the Z boson mass, $\alpha_s(m_Z)$, the direct measurement of its running with Q in the TeV region is also of high interest. The reason is that this running is generically modified in the presence of new strongly interacting particles as predicted by many scenarios of new physics beyond the Standard Model (bSM), such as by squarks and gluinos in supersymmetry, or top partners in composite Higgs models. These modifications are for example crucial in scenarios where the strong and electroweak interactions are unified at very high scales [70].

The effects of such new bSM degrees of freedom are illustrated in Fig. 6, taken from [71], which shows how $\alpha_s(Q)$ is affected by new colored particles for different representations. In this example, a mass of 500 GeV has been assumed by the bSM particles belonging to new strongly interacting multiplets. If such new states are light enough, they could lead to visible effects in the
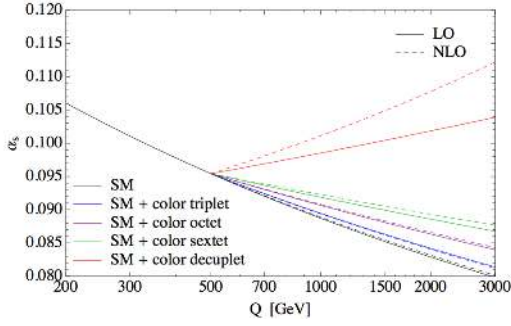
$H_{T,2}/2$	MSTW2008: $\Delta\alpha_s(M_Z) \times 1000$				
(GeV)	$\alpha_s(M_Z)$	exp	PDF	NP	scale
300–420	0.1157	± 15	± 14	± 19	$^{+53}_{-0}$
420–600	0.1153	± 11	± 14	± 18	$^{+57}_{-0}$
600–1000	0.1134	± 13	± 16	± 19	$^{+52}_{-0}$
1000–1680	0.1147	± 29	± 17	± 18	$^{+63}_{-11}$
300–1680	0.1150	± 10	± 13	± 15	$^{+50}_{-0}$

Figure 6: Left: the running of $\alpha_s(Q)$ is generically modified in the presence of new strongly interacting particles as predicted by many bSM scenarios, where 500 GeV mass has been assumed for the new-physics multiplets [71]. Right: the running of $\alpha_s(Q)$ in the TeV scale can be directly determined from LHC processes such as multijet production, in this case we show the CMS 8 TeV analysis [72].

running of $\alpha_s(Q)$ within the LHC range. Conversely, precision measurements of $\alpha_s(Q)$ in the TeV range could be of use to derive stringent model-independent bounds on bSM scenarios containing strongly interacting sectors.

Direct measurements of $\alpha_s(Q)$ in the TeV range can be obtained from processes such as inclusive jet, dijet, and multijet production, as well as top quark pair production in the tail of the $m_{t\bar{t}}$ distribution, which are both sensitive to the value of the strong coupling and lead to sizable event rates in the TeV region. For instance, in Fig. 6 (right) we show the CMS measurement of $\alpha_s(Q)$ from the multijet cross sections at 8 TeV [72] using NLO QCD calculations and MSTW20018 as input PDF set. By restricting the input data used in the fit to separate bins of the $H_{T,2}/2$ kinematic variable, one can effectively measure $\alpha_s(Q)$ for increasing values of Q and thus validate its running by comparing it to the SM predictions. While the current results are limited by the scale uncertainties of the NLO calculation as well as by statistics in the TeV region, future extractions based on NNLO QCD and in a much higher integrated luminosity should be in the position of providing stringent tests of bSM scenarios where the running of $\alpha_s(Q)$ is modified as compared to the QCD prediction.

$\alpha_s(m_Z)$ from electron-positron collisions. The strong coupling can also be determined from high-energy e^+e^- collisions, by exploiting how the pattern of QCD radiation is modified in these collisions once $\alpha_s(m_Z)$ is varied. Specifically, a number of the so-called event shapes such as the thrust or the C-parameter have been in the last years used to extract $\alpha_s(m_Z)$ from LEP measurements. The main benefit of this process is that it is experimentally very clean, and that one has good control over the perturbative calculation including resummation, with recent extractions being based on NNLO+N^{3}LL theory. On the other hand, the extraction of $\alpha_s(m_Z)$ from event shapes requires a precise modeling of the hadronisation mechanism of quarks and gluons (and related non-perturbative effects) in order to connect the perturbative calculation with the LEP cross sections.

Two recent determinations of the strong coupling constant from event shapes [73, 74], based on the Soft-Collinear Effective Theory (SCET) formalism, find the following results:

$$\alpha_s(m_Z) = 0.1135 \pm 0.0011 \qquad \text{(Thrust)}, \qquad (3.3)$$

$$\alpha_s(m_Z) = 0.1123 \pm 0.0015 \qquad (\mathrm{C - parameter}), \tag{3.4}$$

so rather smaller than the PDG average. The reason for these differences is still under investigation. One possible reason could be related to the treatment of non-perturbative effects, which are more challenging to control than the perturbative part of the calculation where residual MHO corrections appear to be quite small.

4. QCD static energy *(A. Vairo)*

Lattice QCD provides a potentially very accurate source of α_s [75], see Sec. 5. Indeed among the determinations quoted by the Particle Data Group [7], the most precise ones are lattice determinations. Among the lattice determinations, the extraction of α_s from the QCD static energy is particularly attractive as the perturbative expansion of this quantity is very accurately known as well as its lattice determination.

Lattice determinations of the QCD static energy have started since the inception of lattice QCD itself. The QCD static energy, $E_0(r)$, is the energy possessed by a static quark and a static antiquark located at a distance r. Its expression in Minkowski spacetime is [76, 77, 78, 79]

$$E_0(r) = \lim_{T \to \infty} \frac{i}{T} \ln \left\langle \mathrm{Tr\,P} \exp \left\{ ig \oint_{r \times T} dz^\mu A_\mu(z) \right\} \right\rangle, \tag{4.1}$$

where the integral is over a rectangle of spatial length r and time length T; $\langle \ldots \rangle$ stands for the path integral over the gauge fields A_μ and the light-quark fields, P is the path-ordering operator of the color matrices (fields are time ordered) eventually traced and g is the QCD gauge coupling ($\alpha_s = g^2/(4\pi)$).

In the short range $r\Lambda_{\mathrm{QCD}} \ll 1$, for which $\alpha_s(1/r) \ll 1$, $E_0(r)$ may be computed as a perturbative expansion in α_s (evaluated at a typical scale of order $1/r$; at three loops and higher, however, also couplings at the lower energy scale α_s/r show up):

$$E_0(r) = \Lambda - \frac{4\alpha_s}{3r}(1 + \ldots), \tag{4.2}$$

where Λ is a constant and the dots stand for higher-order terms. The expansion of $E_0(r)$ in powers of α_s has been computed at order $\alpha_s^4/r \times \ln \alpha_s$ in [80, 81], at order α_s^4/r in [82, 83], at order $\alpha_s^5/r \times \ln \alpha_s$ in [84], all orders $\alpha_s^{4+n}/r \times \ln^{1+n} \alpha_s$ (N²LL accuracy) have been computed in [85], and all orders $\alpha_s^{5+n}/r \times \ln^{1+n} \alpha_s$ (N³LL accuracy) have been computed in [86]. A compact summary of the perturbative expression of $E_0(r)$ can be found in [87].

In lattice regularization Λ includes a linear divergence due to the self-energy $\sim \alpha_s(1/a)/a$, with a the lattice spacing. In dimensional regularization the linear divergence vanishes, but the perturbative expansion of $E_0(r)$ is affected by a renormalon ambiguity of order Λ_{QCD} [88, 89]. The renormalon ambiguity reflects in the poor behaviour of the perturbative series, which may be cured by subtracting the renormalon from the perturbative series and suitably redefining the constant Λ.

If we are interested in (4.2) just for extracting α_s, then the relevant information is encoded in the slope of the static energy, i.e., the force

$$F(r) = \frac{d}{dr} E_0(r). \tag{4.3}$$

11

The force does not depend on Λ. In lattice regularization it is not affected by the linear self-energy divergence and it is free from the renormalon of order Λ_{QCD}. The continuum perturbative expansion of the force shows, therefore, a convergent behaviour (at least up to three loops). In order to compute α_s, one may compare the perturbative continuum expression of the force with its lattice determination. However, a precise direct lattice computation of the force is challenging (see also below), while an accurate determination of $E_0(r)$ is much easier, for it amounts at extracting the exponential fall off of a static Wilson loop. Hence an alternative strategy is to integrate the perturbative continuum expression of the force over the distance, obtaining back the static energy (see also [90]),

$$E_0(r) = \int_{r_*}^{r} dr' F(r'), \tag{4.4}$$

up to an irrelevant constant determined by the arbitrary distance r_*, which can be reabsorbed in the overall normalization when comparing finally with lattice data. Equation (4.4) amounts effectively to a rearrangement of the perturbative expansion of the static energy. The integration in (4.4) can be done (numerically) keeping the strong coupling that appears in the perturbative expansion of the force running at a natural scale of the order of the inverse of the distance.

Whatever strategies one pursues, the comparison of the perturbative expression of the QCD static energy or the force to lattice QCD determinations provides with (at least) three-loop accuracy the QCD strong coupling α_s at a typical scale that is large enough for perturbative QCD to work and smaller than the inverse lattice spacing $1/a$. This means that the distance range of the QCD static energy explored by lattice QCD that is relevant for the extraction of α_s goes from about 0.2 fm to about 0.05 fm or slightly below. Hence, the QCD static energy provides an accurate determination of α_s at a low energy scale, typically about 1.5 GeV, for which it has very few competitors (one of these is the extraction of α_s from the τ decay, as the mass of the τ is about 1.777 GeV, see Sect. 2). This gives to this determination a value in itself and adds to its relevance, regardless of the final precision in the determination of $\alpha_s(m_Z)$. Nevertheless, the precision in the final determination of $\alpha_s(m_Z)$ is also competitive with other determinations. One of the challenges in extracting α_s from the QCD static energy is to move the distance range towards shorter ones in order to be deeper in the perturbative regime and reduce uncertainties originating from not included higher-order terms, keeping at the same time sufficiently away from the minimal lattice distance, a.

Status. Precision determinations of α_s from the QCD static energy have started in quenched QCD with Ref. [90]. The precision of the data allowed computing numerically the derivative of the static energy and hence the force: α_s was computed from the force. More recent pure gauge theory ($N_f = 0$) determinations can be found in [91, 92].

Static-energy determinations with 2 flavors are in [93, 94, 95] and with 2+1 flavors in [96, 97]. A summary of these latest results is in [98]. The most recent analysis of the static energy with 2+1 flavors is in [99, 100]. Considering (somewhat long) distances up to about 0.35 fm to extract α_s, it obtains results that are consistent with the ones in [96, 97], but with larger final errors, see also Fig. 11.

The determination of [97] is based on the perturbative expression (4.4) computed up to N^2LL accuracy and compared with 2+1 flavors lattice data (strange quark mass at its physical value and pion mass at 160 MeV) for $\beta = 7.373$, 7.596 and 7.825 in the range from 0.05 fm to 0.14 fm. The

result is

$$r_1\Lambda_{\overline{\text{MS}}} = 0.495^{+0.028}_{-0.018}. \tag{4.5}$$

Taking the lattice scale $r_1 = 0.3106 \pm 0.0017$ fm from [101], the result translates into

$$\Lambda_{\overline{\text{MS}}} = 315^{+18}_{-12} \text{ MeV} \tag{4.6}$$

for three flavors. The above value of $\Lambda_{\overline{\text{MS}}}$ converts into

$$\alpha_s(1.5\,\text{GeV}, n_f = 3) = 0.336^{+0.012}_{-0.008}, \tag{4.7}$$

at the energy scale of 1.5 GeV that corresponds to a distance of about 0.13 fm and is about the largest scale consistent with a three-flavors running. Finally, this value of α_s evolves to the value

$$\alpha_s(m_Z, n_f = 5) = 0.1166^{+0.0012}_{-0.0008}, \tag{4.8}$$

at the Z mass. A comparison of the lattice data for $\beta = 7.825$ with the perturbative expression is shown in Fig. 7. In the considered distance range, non-perturbative corrections, which would manifest themself as power corrections in r, are consistent with zero.
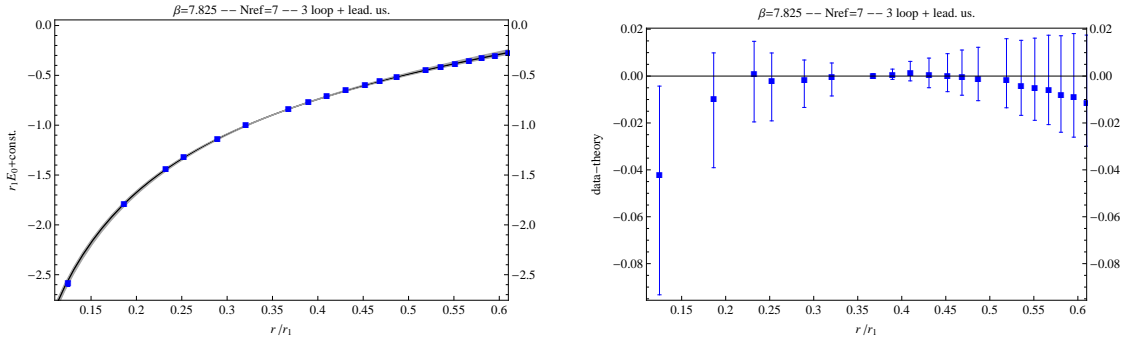

Figure 7: Left panel: Lattice data of the QCD static energy for $\beta = 7.825$ compared with the N^{2}LL perturbative expansion (equivalent to 3 loops plus leading ultrasoft resummation) evaluated for $r_1\Lambda_{\overline{\text{MS}}} = 0.495^{+0.028}_{-0.018}$ (the thin grey band reflects the uncertainty). Right panel: The same lattice data with the perturbative expression subtracted. The error bars are obtained by adding, in quadrature, the errors of the lattice data and the uncertainty of the perturbative expression due to the variation of $r_1\Lambda_{\overline{\text{MS}}}$. The normalization constant in the difference between lattice and perturbative data has been fixed on the seventh point. Data from [97].

A similar analysis has been done in [97] with the force. However, the numerical derivatives of the static energy add to the uncertainties of the strong coupling determination, which, done in this way, turns out to be consistent, but less accurate, than the direct determination from the static energy presented above.

Perspectives. The determination of α_s from the QCD static energy has still room for improvement and will face in the near future interesting challenges. In the following we list some of them.

Not all of the available theoretical information on the short-distance static energy has been used: in particular, presently available data do not seem sensitive neither to the N^{3}LL expression of the static energy, nor to short-range non-perturbative effects (e.g., condensates $\sim r^3\langle g^2\mathbf{E}(0)^2\rangle$, or correlators $\sim r^2 \int_0^\infty dt\langle g\mathbf{E}(t)\cdot g\mathbf{E}(0)\rangle$, where $\mathbf{E}$ is the chromoelectric field). One question is

13

then if lattice data at shorter distances and more accurate will become sensitive to these effects. It should be mentioned that an assessment of the size of the non-perturbative contributions to the static energy will have a major impact on quarkonium physics.

Forthcoming lattice computations with 2+1+1 flavors will naturally raise the question of how much the data for the static energy will turn out to be sensitive to the charm mass and of how much this will affect the extraction of α_s. The region around the charm quark mass, $(1.5\,\text{GeV})^{-1} \approx 0.13\,\text{fm}$, and below is indeed the region from where α_s from the static energy mostly comes.

More precise lattice data may also allow for a competitive determination of α_s directly from the force, as it was done long ago in quenched QCD [102], and as it may be possibly done also by looking to loop functions different from the static Wilson loop.

α_s from the static energy at very short distances. As mentioned above, one may look at the static energy at very short distances to minimize the effect of unknown higher-order terms, which include perturbative and non-perturbative contributions, and to have a better behaved series. This may certainly represent an improvement with respect to present determinations, but one should also realize that the range from 0.05 fm to 0.14 fm used in [97] already shows a well behaved perturbative series, agreement with data and a stable result with respect to (adding/subtracting) lattice data, renormalization scale, etc.

A new set of data from a short-distance determination of the static energy in the range from about 0.02 fm to 0.18 fm on a lattice with 2+1 flavors will be presented in Ref. [103]. At short distances finite volume effects are irrelevant, as confirmed by previous analyses. A possible issue is however that at small lattice spacings the Monte Carlo evolution of the topological charge freezes. Although a thoroughly investigation is still to be done, the analysis performed in [104] does not show for the considered observables any sensitivity if the topological charges 0, 1 and 2 are considered.

Preliminary results are shown in Fig. 8. The data prefer a somewhat lower value of α_s with respect to the PDG average, but consistent with the result (4.8).
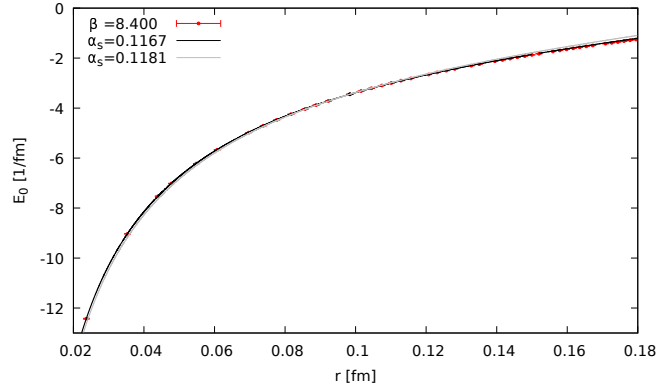

Figure 8: Preliminary lattice data for the static energy at $\beta = 8.4$ from [103] compared with the N^{2}LL perturbative expression, for $\alpha_s(m_Z, n_f = 5) = 0.1167$ and for $\alpha_s(m_Z, n_f = 5) = 0.1181$ (PDG value [7]).

Charm mass effects. Since the charm mass is larger than Λ_{QCD}, at distances comparable with the inverse of the charm mass or shorter, charm-mass effects may be computed in perturbative QCD.

Indeed, the effect of a charm mass loop to the QCD static energy is well known (see Ref. [105]). As mentioned above, a finite charm mass contributes to the static energy at distances where one mostly compares lattice data with perturbative QCD, and eventually extracts α_s. Similarly, charm mass loops are relevant for precision bottomonium physics, because the typical momentum transfer inside the $\Upsilon(1S)$ is about the charm mass.

In Fig. 9, we compare at one loop the static energy in perturbative QCD with α_s running with 3 flavors, 4 flavors and with 4 flavors plus the one-loop contribution of a massive charm. At large distances, the charm decouples, and the static energy is effectively described by a 3 flavors α_s. At short distances, the charm may be considered massless, and the static energy is effectively described by a 4 flavors α_s. Accurate lattice data should be sensitive to this transition and, in particular, to the intermediate region where the static energy is best described by a charm with a finite mass.
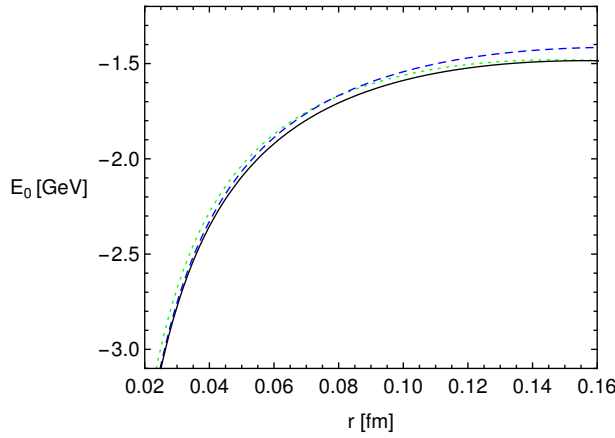
Figure 9: Dashed blue: massless charm (case of 4 active flavors); dotted green: infinitely heavy charm (case of 3 active flavors); black: massive charm at 1 loop ($\overline{\text{MS}}$ mass taken to be 1.237 GeV).

$\boldsymbol{\alpha_s}$ **from the force.** Precise lattice data of the QCD static energy may allow for a precise determination of the force by interpolating the lattice points and numerically performing the derivatives. An alternative direct determination of the force could come from computing a Wilson loop with a chromoelectric field insertion [106, 98]:

$$F(r) = -\lim_{T\to\infty} \frac{\left\langle \text{Tr}\,\text{P}\,\hat{\mathbf{r}} \cdot g\mathbf{E}(t,\mathbf{r}) \exp\left\{ ig \oint_{r\times T} dz^\mu A_\mu(z) \right\} \right\rangle}{\left\langle \text{Tr}\,\text{P} \exp\left\{ ig \oint_{r\times T} dz^\mu A_\mu(z) \right\} \right\rangle}. \tag{4.9}$$

This quantity has been computed in the context of determining the quarkonium potentials on the lattice in Ref. [107]. However, a dedicated study with the aim of extracting α_s is still to be done. In particular, the lattice version of $g\mathbf{E}(t,\mathbf{r})$ needs to be properly renormalized.

5. Lattice determinations *(R. Sommer)*

Lattice gauge theory is a non-perturbative formulation of QCD, which allows to evaluate the Euclidean path integral by a Monte Carlo "simulation". The process starts from discretizing space-time on a hypercubic lattice with lattice spacing a and thus a momentum cutoff of $|p_\mu| \le \pi/a$. Due

to the large number of degrees of freedom and the fermionic nature of quark fields, the Monte Carlo process requires considerable effort and both the simulated space-time $T \times L^3$ and the spacing a are restricted. Although lattice ensembles with $L/a = \mathcal{O}(100)$ are possible nowadays, even this number sets limits to what can be done, which we will discuss shortly.

First, let us give a broad characterization of the lattice methods for extracting the QCD coupling. Indeed there are several methods. Their differences are at least as big as the difference of a phenomenological extraction from DIS vs. from τ decays. It is important and not too difficult to have a rough grasp of these differences. For more details we refer to [75].

In general, one performs a Monte Carlo evaluation of the path integral representation of observables (correlation functions) for a few suitably chosen values of

$$ L/a, \ T/a, \ g_0, \ \{am_i, \ i = 1 \ldots N_f\}. \tag{5.1} $$

Here L/a is the number of points of the world in each space dimension, T (often bigger than L) is the extent of the time axis, g_0 is the bare coupling of the theory and am_i are the bare quark masses. Think now of the theory with just the lightest three quarks and isospin symmetry, $m_1 = m_2$. The first step is to obtain the relation between the bare parameters, g_0, am_1, am_3 and three hadronic, low energy quantities, which are conveniently chosen to be the masses of pion and kaon as well as a leptonic decay constant, which we here just take to be f_π.[1] More precisely, the functions

$$ F_1(g_0, am_1, am_2) = \frac{m_\pi}{f_\pi}, \tag{5.2} $$

$$ F_2(g_0, am_1, am_2) = \frac{m_K}{f_\pi}, \tag{5.3} $$

$$ F_3(g_0, am_1, am_2) = a f_\pi, \tag{5.4} $$

are determined for a few values of their arguments. Then, at fixed g_0, one finds by appropriate fits/extrapolations values $\mu_i^*(g_0)$ such that $F_1(g_0, \mu_1(g_0), \mu_2(g_0)) = m_\pi^{\text{QCD}}/f_\pi^{\text{QCD}}$ and analogous for F_2. Here the label QCD refers to PDG numbers corrected for isospin violating and electromagnetic effects. F_3 is then used to determine the lattice spacing, $a(g_0) = F_3(g_0, \mu_1(g_0), \mu_2(g_0))/f_\pi^{\text{QCD}}$. The latter step is called scale setting because from now on all dimensionful quantities which are originally just defined in units of the lattice spacing a can now be expressed in physical units. All of this has to be done in volumes which are large enough such that finite size effects on the used hadron masses and decay constants are negligible. Fortunately finite size effects are quite well understood and asymptotically decrease exponentially $\sim \exp(-m_\pi L)$. Choosing $m_\pi L \gtrsim 4$ is sufficient. Such a bound imposes a limitation to the lattice spacings available in large volume. For numbers one has to take into account that simulations can also be carried out at pion masses larger than in Nature. What is roughly realized nowadays is

$$ a \gtrsim 0.04 \, \text{fm} \tag{5.5} $$

in a "large volume".

---

[1]Pion and kaon masses are clearly the observables of choice to fix the light quark masses. However, for fixing the bare coupling or equivalently the overall scale of QCD, the nucleon mass would be more natural. Unfortunately it is difficult once precision is required. See [108] for details.
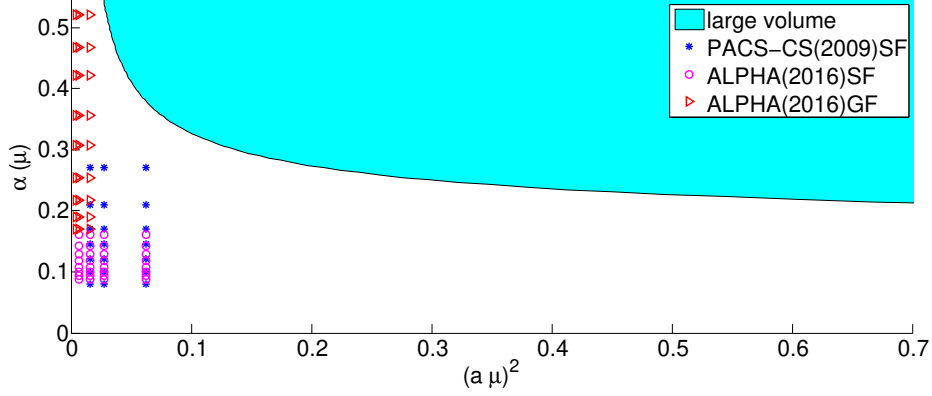
16

Figure 10: The plane $\alpha_{\overline{MS}}^{(3)}(\mu)$ against the scale μ in lattice units. a is the lattice spacing and the blue region corresponds to the rough bound $a > 0.04$ fm. Note that the continuum limit is approached by extrapolations with $a\mu \ll 1$. The points on the left correspond to actual Monte Carlo simulations in category (III).

5.1 Methods for the strong coupling.

The general method for extracting $\alpha_{\overline{MS}}$ with the help of lattice QCD is to consider a short-distance, one-scale, observable with an expansion (an $\alpha_{\overline{MS}}(\mu)^0$ term can always be subtracted)

$$\mathcal{Q}(\mu) = c_1\alpha_{\overline{MS}}(\mu) + c_2\alpha_{\overline{MS}}(\mu)^2 + \cdots. \tag{5.6}$$

The observable is computed by lattice QCD and applying the perturbative expansion with c_{n_l+1} known is denoted by a determination at n_l loops. It means that for the effective coupling

$$\alpha_{\text{eff}} = \mathcal{Q}/c_1 \tag{5.7}$$

the $n_l + 1$ loop β-function is known. We will mostly have $n_l = 2$, but for the static potential $n_l = 3$ (with some complications, see Sect. 4) holds.

Advantages.   An important advantage of taking $\mathcal{Q}$ from lattice QCD compared to using experimental data is that one is automatically in the Euclidean where perturbation theory works and no hadronisation corrections, duality violations etc. are a concern. Furthermore one has the freedom to design suitable observables.

Disadvantages.   In practice, lattice QCD simulations are restricted to $N_f = 4$ quarks at the most, because the b-quark is simply too heavy. One relies on including the heavy flavors, mostly including the charm, by perturbation theory, using 4-loop matching and 5-loop running in the $\overline{MS}$ scheme [109, 6, 5, 110, 111, 112, 2, 3, 1, 113]. Worries that this might compromise the error estimates of the results have recently been removed by a non-perturbative study [114].

We turn to the announced different categories.

(I) Continuum-limit observables in large volume.   The most straightforward strategy is to take a finite observable $\mathcal{Q}$ which depends on a single large momentum scale μ and which is defined in

17

a large volume (i.e., large enough such that finite volume effects can be neglected). One can then (and needs to) take the continuum limit

$$\mathscr{Q}(\mu) \equiv \lim_{a \to 0} \mathscr{Q}_{\text{lat}}(a, \mu) \text{ with } \mu \text{ fixed} . \tag{5.8}$$

In practice this is done by an extrapolation in $a\mu \to 0$ using the structural information from Symanzik's effective theory [115] of lattice artefacts that (assuming $\mu \gg \Lambda$)

$$\mathscr{Q}(\mu) - \mathscr{Q}_{\text{lat}}(a, \mu) \overset{a\mu \to 0}{\sim} a^2 \mu^2 . \tag{5.9}$$

Here, the challenge is that one wants μ to be high such that $\alpha_{\overline{\text{MS}}}(\mu)$ is small and the expansion Eq. (5.6) is precise and at the same time $a\mu$ small because of Eq. (5.9). Recalling Eq. (5.5) one is usually in the blue shaded region of Fig. 10 and it is difficult to extrapolate when $\alpha_{\overline{\text{MS}}}$ is small, say $\alpha_{\overline{\text{MS}}} \le 0.3$. One has to compromise between the two requirements. At this conference, Peter Petreczky reported about recent progress using this method.

(II) Lattice observables at the cutoff. There is also the possibility to consider lattice observables involving distances of a few lattice spacings, which are not related to a continuum observable. The prominent examples are rectangular Wilson loops $W(r,t)$ of extent $r \times t$ with $r = am$ and $t = an$, keeping the integers n, m fixed as one takes the limit $a \to 0$; the loops shrink to size zero in the limit. Still such observables have an expansion

$$W(na, ma) \overset{g_0 \to 0}{\sim} \sum_{k \ge 0} c_{m,n}^{(k)} g_0^{2k} \overset{a \to 0}{\sim} \sum_{k \ge 0} \hat{c}_{m,n}^{(k)} \bar{g}_{\overline{\text{MS}}}^{2k}(1/a) , \tag{5.10}$$

where in the second step use is made of the relation between the bare coupling and a renormalized coupling at the cutoff scale, $g_0^2 = \bar{g}_{\overline{\text{MS}}}^2(1/a) + \mathscr{O}(\bar{g}^4)$.

We note two features of this approach: *(i)* Lattice perturbation theory has to be used and there is less experience with the size of higher-order terms (even after tadpole improvement [116]) and the available loop orders are often lower than for continuum perturbation theory. *(ii)* Lattice artefacts can only be separated from perturbative corrections in Eq. (5.10) by assuming some functional form and fitting to it.

(III) Continuum-limit observables in small volume and step scaling. Early on, there was the idea [117] of using the freedom in the definition of $\mathscr{Q}(\mu)$ to consider finite volume quantities, e.g. in L^4 geometries. Then the renormalization scale in $\alpha_s(\mu)$ is

$$\mu = 1/L , \tag{5.11}$$

and any other dimensionful parameter present in the definition of $\mathscr{Q}(\mu)$ is in a fixed relation to (scaled with) L. The advantage is that now $\mu a = a/L$ can easily be taken to $a/L = 1/8 \ldots 1/32$ or smaller. However, a number of steps are needed to connect recursively

$$\mu_0 \to s\mu_0 \to s^2\mu_0 \to \ldots \to s^N\mu_0 , \tag{5.12}$$

and in each step a few different lattice spacings a have to be simulated to take the continuum limit. The start value μ_0 has to be taken such that the lattice spacings are known in fm through

a large volume scale setting sketched above. Thus one typically starts with $\mu_0 = \mathscr{O}(1\,\mathrm{fm}^{-1}) = \mathscr{O}(200\,\mathrm{MeV})$ and needs e.g. $s = 2, N = 9$ in order to be beyond the Z mass, where perturbation theory can be applied with great confidence. Indeed, at significantly lower energies, one has to be more careful, as seen explicitly by the investigation in [118]. There a family of schemes all with a well-behaved three-loop β-function were studied non-perturbatively. Depending on the exact choice of scheme, truncation errors of perturbation theory were found to be large at the level of precision that we are discussing for $\alpha_{\overline{\mathrm{MS}}}$. At this conference, Alberto Ramos presented a recent precise three-flavor computation using this method. For details we refer to his contribution.

5.2 Towards the 2019 FLAG review.

The Flavour Lattice Averaging Group (FLAG) formed a working group (R. Horsley, T. Onogi, R.S.) on α_s in 2011 and first included determinations of $\alpha_s(m_Z)$ in its review in 2013 [119]. An update appeared in 2016 [75]. Presently we are preparing the 2019 edition. Here I will report on its **preliminary** status and give a preliminary world average. However, first I will roughly explain the algorithm to arrive at averages. It has similarities to PDG but still differs significantly from the PDG practice. The main difference is that FLAG formulates a set of criteria, which computations have to pass in order to enter the average of a given quantity of phenomenological interest [75].

Criteria. We cite here from the present draft of the new FLAG review:
The major sources of systematic error are common to most lattice calculations. These include, as discussed in detail below, the chiral, continuum and infinite-volume extrapolations. To each such source of error for which systematic improvement is possible we assign one of three coloured symbols: green star, unfilled green circle ... or red square. These correspond to the following ratings:

- ★ *the parameter values and ranges used to generate the datasets allow for a satisfactory control of the systematic uncertainties;*
- ○ *the parameter values and ranges used to generate the datasets allow for a reasonable attempt at estimating systematic uncertainties, which however could be improved;*
- ■ *the parameter values and ranges used to generate the datasets are unlikely to allow for a reasonable control of systematic uncertainties.*

The appearance of a red tag, even in a single source of systematic error of a given lattice result, disqualifies it from inclusion in the global average.

The last sentence is a first difference to the PDG procedure.

For the computations of α_s, the criteria for chiral and infinite volume extrapolations are relaxed as they do not play a dominant role. Instead criteria on *perturbative behaviour* and *renormalization scale* try to make sure that the computation is at reasonable high μ, the perturbative knowledge is sufficiently good (i.e., n_l, the number of loops, is sufficiently high) and μ could be varied over some range in order to confirm the perturbative μ-dependence. We do not have the space here to discuss this in detail, but the general idea is that these criteria try to make sure that the available Monte Carlo data have a few points located sufficiently low in the landscape of Fig. 10, while the continuum limit criterion requires to not be too far on the right. Details are listed in [75]; changes in FLAG 2019 will be minor.

19

α_s from different methods. We now discuss the status of the results for $\alpha_{\overline{\text{MS}}}^{(5)}(m_Z)$. In Tab. 2 all relevant computations are listed. They are organized according to the different methods, namely the different observables $\mathscr{Q}$ used. The last column lists the loop order defined above. We go through the different methods, following the classification (I-III) of before.

(I) Continuum-limit observables in large volume. There is a large number of different methods. They share the necessity for finding a compromise between large μ and small $a\mu$. In the cases where computations qualify for taking an average (i.e., there is no red square), we perform a weighted average of the different results. This yields the mean of the quoted pre-ranges in Tab. 2. According to our judgement the uncertainties are dominantly systematic. They are due to the truncation error of perturbation theory, whether ordinary higher order or non-perturbative effects. The question is always whether the values of μ are high enough. We just estimate the perturbative truncation error and take this as the uncertainty of the pre-range. Comparing with the errors of the individual collaborations one sees that we are somewhat more conservative in our estimate of the perturbative uncertainty, which seems a good strategy if one wants to arrive at a safe final range. The individual methods are (we partially have to simplify)

1. Q-$\bar{Q}$ potential: $\quad \mathscr{Q}(\mu) = r^2 F_{\text{static}}(r), \quad \mu = 2/r$, where $F_{\text{static}}(r)$ is the force between static quarks defined by the large-t behaviour of Wilson loops $W(r,t)$. Note that n_l is 3 but $n_l > 3$ terms proportional to $\log \alpha$ are also known. Indeed, at fixed order perturbation theory, starting from three loops, there are infrared divergences. As mentioned in Sect. 4 and references cited there, these divergences cancel once contributions from the scale α_s/r are resummed, leaving terms such as $\alpha^4 \log \alpha$ in $\mathscr{Q}(\mu)$, which, in turn, can be resummed to all orders via renormalization group equations.

2. vacuum polarization: $\quad \mathscr{Q}(\mu) = D(Q^2), \quad \mu^2 = Q^2$, with D the Adler function derived from $\Pi_{ij,V+A}^{\mu\nu}(q)$ (Eq. (2.1)) at Euclidean q and $i \neq j$. This method does not yet enter the average as the presently best rating is (○ ★ ■) [120].

3. Hl current, two points: moments of heavy-light pseudoscalar-current two-point functions. Heavy quarks of masses around the charm and heavier are used. This method has attracted a lot of attention. Different discretizations are used that allow also to compare the continuum-limit moments before the extraction of α_s. There is quite good agreement, but some tensions exist.

4. gluon-ghost vertex: using gauge fixing, the momentum-space vertex is used. This method does not yet enter the average as the continuum limit criterion is not passed.

5. Dirac eigenvalues: $\quad \mathscr{Q}(\mu) = \frac{\partial \log(\rho(\lambda))}{\partial \log(\lambda)}, \quad \mu = \lambda$ with $\rho(\lambda)$ the spectral density of the massless Dirac operator. Also this newly introduced method [121] does not yet pass the continuum-limit criterion.

(II) Lattice observables at the cutoff. In this category small ($m, n \leq 3$) Wilson loops

$$\mathscr{Q}(\mu) = W(ma, na), \quad \mu = k/a$$

and functions thereof (e.g. $\log(W(a,a))$ are used. The scale factor k is adjusted to have better apparent convergence of PT. Our estimate of perturbative uncertainties is somewhat bigger than the one of the collaborations.

(III) Continuum-limit observables in small volume and step scaling. Finite volume couplings (with Dirichlet boundary conditions in time) are used and their μ-dependence is traced to $\mathcal{O}(100\,\text{GeV})$ by step scaling. Perturbative errors are negligible and statistical errors of the many Monte Carlo computations dominate. In [122] the freedom of choice for the definition of the coupling is used to actually impose one definition at energies smaller than 4 GeV and a different one for higher energies. This reduces overall uncertainties.
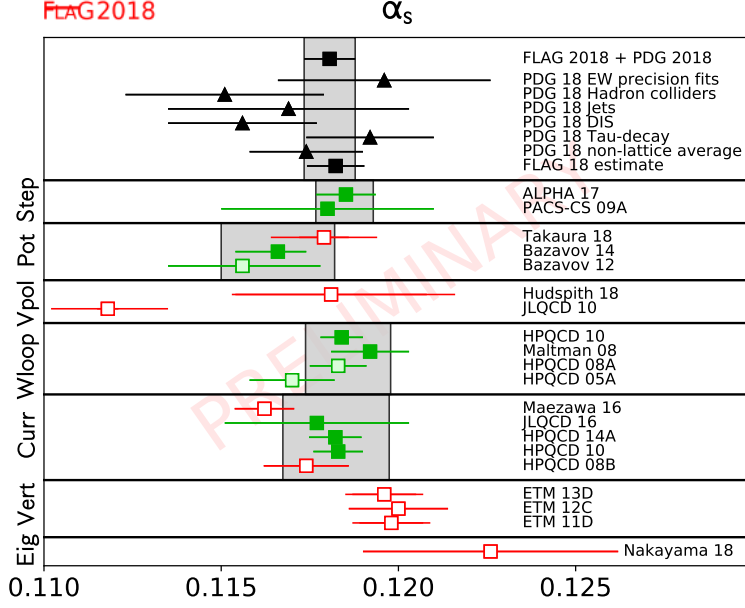

Figure 11: $\alpha_{\overline{\text{MS}}}^{(5)}(m_Z)$, the coupling constant in the $\overline{\text{MS}}$ scheme at the Z mass. The PDG 18 entries give the outcome of their analysis from various phenomenological categories including their average. The lattice computations with a filled green box symbol have no red box in the previous ratings and therefore qualify for averaging. An open green square means the same but the number does not enter an average because it is superseded by a later more complete computation or it was not published at the September 2018 deadline. Computations with open red squares do not enter the averages because they had at least one red square before.

World average from FLAG. The entries of Tab. 2 are also displayed in Fig. 11. For each method, the gray band shows the pre-average as explained above. We are left with the task to combine those pre-averages. Again we take the central value from their weighted average. However, since the errors of the pre-averages are mostly systematic, we feel that the straight error 0.00057 of the weighted average is too optimistic – it would be correct for independent Gaussian distributions. Instead we use the smallest error of the pre-averages. This yields the **preliminary** result

preliminary: $\alpha_{\overline{\text{MS}}}^{(5)}(m_Z) = 0.11823(81)$ Refs. [123, 129, 97, 131, 127, 124, 128],   (5.13)

and the associated Λ parameter

preliminary: $\Lambda_{\overline{\text{MS}}}^{(5)} = 211(10)$ MeV   Refs. [123, 129, 97, 131, 127, 124, 128].   (5.14)

Collaboration	Ref.	N_f	publication status	renormalization scale	perturbative behaviour	continuum extrapolation	$\alpha_{\overline{\mathrm{MS}}}(M_Z)$	method	n_l
ALPHA 17	[123]	2+1	A	★	★	★	0.11852(84)	step scaling	2
PACS-CS 09A	[124]	2+1	A	★	★	○	0.11800(300)		2
pre-range (average)							0.11848(81)		
Takaura 18	[99, 100]	2+1	P	■	○	○	$0.11790(70)\left(^{+130}_{-120}\right)$	Q-$\bar{Q}$ potential = static energy (sect. 4)	3
Bazavov 14	[97]	2+1	A	○	★	○	$0.11660\left(^{+120}_{-80}\right)$		3
Bazavov 12	[96]	2+1	A	○	○	○	$0.11560\left(^{+210}_{-220}\right)$		3
pre-range with estimated pert. error							0.11660(160)		
Hudspith 18	[125]	2+1	P	○	○	■	$0.11810(270)\left(^{+80}_{-220}\right)$	vacuum polarization	3
JLQCD 10	[126]	2+1	A	■	○	■	$0.11180(30)\left(^{+160}_{-170}\right)$		2
HPQCD 10	[127]	2+1	A	○	★	★	0.11840(60)	Wilson loops	2
Maltman 08	[128]	2+1	A	○	○	★	0.11920(110)		2
pre-range with estimated pert. error							0.11858(120)		
JLQCD 16	[129]	2+1	A	○	○	○	0.11770(260)	Hl current, two points	2
Maezawa 16	[130]	2+1	A	○	■	○	0.11622(84)		2
HPQCD 14A	[131]	2+1+1	A	○	★	○	0.11822(74)		2
HPQCD 10	[127]	2+1	A	○	★	○	0.11830(70)		2
HPQCD 08B	[132]	2+1	A	■	■	■	0.11740(120)		2
pre-range with estimated pert. error							0.11824(150)		
ETM 13D	[133]	2+1+1	A	○	○	■	0.11960(40)(80)(60)	gluon-ghost vertex	3
ETM 12C	[134]	2+1+1	A	○	○	■	0.12000(140)		3
ETM 11D	[135]	2+1+1	A	○	○	■	$0.11980(90)(50)\left(^{+0}_{-50}\right)$		3
Nakayama 18	[121]	2+1	A	★	○	■	0.12260(360)	Dirac eigenvalues	2

Table 2: Results for $\alpha_{\overline{\mathrm{MS}}}(M_Z)$ from simulations that use $2+1$ or $2+1+1$ flavours of quarks. A weighted average of the pre-ranges gives $0.11823(57)$, using the smallest pre-range gives $0.11823(81)$ and the average size of ranges as an error gives $0.11823(128)$.

The PDG has unfortunately not updated its world average since its 2016 value

$$\alpha_{\overline{\mathrm{MS}}}^{(5)}(m_Z) = 0.1174(16), \quad \text{PDG 2016, non-lattice [136]}. \tag{5.15}$$

That number originates from the different pre-averages listed in the upper box of Fig. 11. We can now add the information from the lattice and arrive at an average

$$\text{preliminary: } \alpha^{(5)}_{\overline{\text{MS}}}(m_Z) = 0.11806(72), \quad \text{FLAG 2018 + PDG 2018/2016} \tag{5.16}$$

of PDG non-lattice and FLAG lattice (weighted average). The error is reduced significantly compared to FLAG 2016 and PDG 2016 and almost as small as PDG 2014. Unfortunately Eq. (5.16) does not yet contain the interesting new non-lattice analyses discussed at this conference.

5.3 Further progress

Here I collect some lessons which I have learned during the period when I was involved in forming and discussing a world average for α_s.

The basic problem is simple and has been spelled out often, phrased in varying words. In order to have a precise value with an error that can be estimated by perturbation theory itself, large energy scales μ have to be reached and theory assumptions have to be kept at a minimum. I think that we will not make further progress if we include complicated processes, where non-perturbative contributions have to be fitted or removed by complicated analyses in order to make lower energies accessible. Dealing with non-perturbative physics is always based on assumptions – if only where the expansion in $1/\mu$ applies and lowest-order terms $(1/\mu)^{N_{\min}}$ dominate.

We should therefore separate the determination of α_s at high enough μ, simple theory, from tests of perturbation theory, with resummations, studies of higher-twist contributions, etc.

The concept of criteria introduced by FLAG is very useful in this respect and I would advocate to consider such a procedure for phenomenological determinations. One should at least consider a criterion on minimum values of μ, paired with sufficiently high perturbative order. In FLAG these are the "renormalization scale" / "perturbative behaviour" criteria.

I personally also think that the criteria of FLAG need to be made more strict as time goes on. This is necessary to avoid situations where complicated procedures, involving e.g. separate estimates of perturbative errors (see above) are needed to arrive at a safe range.

Finally, it seems that the limit of lattice determinations of α_s is not yet reached; I believe a factor two reduction in the error is possible with some variation of the developed techniques and some dedication. A rather tough limitation, which is beyond such a factor of two, may be the inclusion of electromagnetic effects. They dominantly (by far) enter in the process of scale setting. At present one essentially uses models for relating Nature at low energy to pure QCD with electromagnetic interactions removed. A typical estimate of the precision is at the level significantly below a % for, e.g., f_π, defined in pure QCD related to $\pi \to \ell\nu + \gamma$'s decays in Nature [136]. Uncertainties due to that step can be translated directly into those of the 3-flavour Λ-parameter which is at the level of 4% right now. In other words, there is still some room before that limit becomes relevant.

6. Final discussion

The spectacular progress achieved in higher-order QCD calculations has made possible to predict many observables with an impressive NNLO accuracy, reaching even the N^{3}LO for fully inclusive quantities such as R_Z and $R_{\tau,V+A}$, as well as for the static energy. With this improved

theoretical control, rather clean and precise determinations of the strong coupling have come out in a rich variety of energy scales. At the same time, high-precision lattice computations have been able to control the continuum limit in α_s determinations with NNLO accuracy up to energies around the Z mass. The addition of novel LHC processes directly sensitive to α_s, and for which NNLO QCD calculations are available, have allowed several recent determinations from global PDF fits with small uncertainties; being able to estimate the theory errors associated to these determinations arising from MHO is now essential to make further progress in this direction.

The most precise determinations of $\alpha_s(m_Z)$ are currently obtained from lattice simulations. The FLAG lattice average in Eq. (5.13) clearly dominates any world average with non-lattice results, making manifest the importance of having a strict and reliable control of lattice and perturbation theory systematics; before averaging the results, FLAG tries to ensure their quality by a set of criteria. The good agreement between the FLAG average and the accurate non-lattice determinations presented in Eqs. (2.3), (2.7) and (3.1) constitutes a highly non-trivial consistency test among results obtained with quite different techniques and physical observables. Still, there remain some results which are quite a bit lower. In this report we mentioned Eqs. (3.3) and (3.4), as well as the ABMP16 result in Fig. 3. These differences need to be better understood.

A precise determination of $\alpha_s(m_Z)$ is of paramount relevance, since it fixes the unique coupling of QCD and, therefore, its predictions for any physical system. Nevertheless, we must also emphasize the very important added value of precisely measuring the strong coupling at different scales. The accurate low-energy determinations from τ decay, in Eq. (2.6), and from a number of lattice determinations such as the QCD static energy, in Eq. (4.7), provide the needed inputs to perform a very significant test of the running of α_s. The beautiful agreement with measurements performed at much higher energies gives a fundamental verification of the asymptotic-freedom property of QCD. In addition, LHC cross sections have also the unique capability of directly measuring the running of $\alpha_s(Q)$ far above the electroweak scale, providing a unique test of the Standard Model and of new strongly interacting sectors at high energies.

Acknowledgments

References

[1] P. A. Baikov, K. G. Chetyrkin, and J. H. Kühn, *Five-Loop Running of the QCD coupling constant*, *Phys. Rev. Lett.* **118** (2017), no. 8 082002, [`arXiv:1606.08659`].

[2] T. Luthe, A. Maier, P. Marquard, and Y. Schröder, *Towards the five-loop Beta function for a general gauge group*, *JHEP* **07** (2016) 127, [`arXiv:1606.08662`].

[3] F. Herzog, B. Ruijl, T. Ueda, J. A. M. Vermaseren, and A. Vogt, *The five-loop beta function of Yang-Mills theory with fermions*, *JHEP* **02** (2017) 090, [`arXiv:1701.01404`].

[4] T. Luthe, A. Maier, P. Marquard, and Y. Schroder, *The five-loop Beta function for a general gauge group and anomalous dimensions beyond Feynman gauge*, *JHEP* **10** (2017) 166, [`arXiv:1709.07718`].

[5] Y. Schroder and M. Steinhauser, *Four-loop decoupling relations for the strong coupling*, *JHEP* **01** (2006) 051, [`hep-ph/0512058`].

[6] K. G. Chetyrkin, J. H. Kuhn, and C. Sturm, *QCD decoupling at four loops*, *Nucl. Phys.* **B744** (2006) 121–135, [`hep-ph/0512060`].

[7] **Particle Data Group** Collaboration, M. Tanabashi et al., *Review of Particle Physics*, *Phys. Rev.* **D98** (2018), no. 3 030001.

[8] P. A. Baikov, K. G. Chetyrkin, and J. H. Kuhn, *Order alpha**4(s) QCD Corrections to Z and tau Decays*, *Phys. Rev. Lett.* **101** (2008) 012002, [`arXiv:0801.1821`].

[9] P. A. Baikov, K. G. Chetyrkin, J. H. Kuhn, and J. Rittinger, *Complete $\mathcal{O}(\alpha_s^4)$ QCD Corrections to Hadronic Z-Decays*, *Phys. Rev. Lett.* **108** (2012) 222003, [`arXiv:1201.5804`].

[10] P. A. Baikov, K. G. Chetyrkin, J. H. Kuhn, and J. Rittinger, *Adler Function, Sum Rules and Crewther Relation of Order $\mathcal{O}(\alpha_s^4)$: the Singlet Case*, *Phys. Lett.* **B714** (2012) 62–65, [`arXiv:1206.1288`].

[11] K. G. Chetyrkin, J. H. Kuhn, and A. Kwiatkowski, *QCD corrections to the e^+e^- cross-section and the Z boson decay rate*, `hep-ph/9503396`. [Phys. Rept.277,189(1996)].

[12] K. G. Chetyrkin, R. V. Harlander, and J. H. Kuhn, *Quartic mass corrections to R_{had} at $\mathcal{O}(\alpha_s^3)$*, *Nucl. Phys.* **B586** (2000) 56–72, [`hep-ph/0005139`]. [Erratum: Nucl. Phys.B634,413(2002)].

[13] **Gfitter Group** Collaboration, M. Baak, J. Cúth, J. Haller, A. Hoecker, R. Kogler, K. Mönig, M. Schott, and J. Stelzer, *The global electroweak fit at NNLO and prospects for the LHC and ILC*, *Eur. Phys. J.* **C74** (2014) 3046, [`arXiv:1407.3792`].

[14] S. Narison and A. Pich, *QCD Formulation of the tau Decay and Determination of Λ_{MS}*, *Phys. Lett.* **B211** (1988) 183–188.

[15] E. Braaten, *QCD Predictions for the Decay of the tau Lepton*, *Phys. Rev. Lett.* **60** (1988) 1606–1609.

[16] E. Braaten, *The Perturbative QCD Corrections to the Ratio R for tau Decay*, *Phys. Rev.* **D39** (1989) 1458.

[17] E. Braaten, S. Narison, and A. Pich, *QCD analysis of the tau hadronic width*, *Nucl. Phys.* **B373** (1992) 581–612.

[18] W. J. Marciano and A. Sirlin, *Electroweak Radiative Corrections to tau Decay*, *Phys. Rev. Lett.* **61** (1988) 1815–1818.

[19] E. Braaten and C.-S. Li, *Electroweak radiative corrections to the semihadronic decay rate of the tau lepton*, *Phys. Rev.* **D42** (1990) 3888–3891.

[20] J. Erler, *Electroweak radiative corrections to semileptonic tau decays*, *Rev. Mex. Fis.* **50** (2004) 200–202, [hep-ph/0211345].

[21] M. Davier, A. Höcker, B. Malaescu, C.-Z. Yuan, and Z. Zhang, *Update of the ALEPH non-strange spectral functions from hadronic τ decays*, *Eur. Phys. J.* **C74** (2014), no. 3 2803, [arXiv:1312.1501].

[22] F. Le Diberder and A. Pich, *Testing QCD with tau decays*, *Phys. Lett.* **B289** (1992) 165–175.

[23] F. Le Diberder and A. Pich, *The perturbative QCD prediction to R(tau) revisited*, *Phys. Lett.* **B286** (1992) 147–152.

[24] A. A. Pivovarov, *Renormalization group analysis of the tau lepton decay within QCD*, *Z. Phys.* **C53** (1992) 461–464, [hep-ph/0302003]. [Yad. Fiz.54,1114(1991)].

[25] **ALEPH** Collaboration, D. Buskulic et al., *Measurement of the strong coupling constant using tau decays*, *Phys. Lett.* **B307** (1993) 209–220.

[26] **ALEPH** Collaboration, R. Barate et al., *Measurement of the spectral functions of axial - vector hadronic tau decays and determination of* $\alpha_s(m_\tau^2)$, *Eur. Phys. J.* **C4** (1998) 409–431.

[27] **ALEPH** Collaboration, S. Schael et al., *Branching ratios and spectral functions of tau decays: Final ALEPH measurements and physics implications*, *Phys. Rept.* **421** (2005) 191–284, [hep-ex/0506072].

[28] M. Davier, A. Hocker, and Z. Zhang, *The Physics of hadronic tau decays*, *Rev. Mod. Phys.* **78** (2006) 1043–1109, [hep-ph/0507078].

[29] M. Davier, S. Descotes-Genon, A. Hocker, B. Malaescu, and Z. Zhang, *The Determination of* α_s *from Tau Decays Revisited*, *Eur. Phys. J.* **C56** (2008) 305–322, [arXiv:0803.0979].

[30] **CLEO** Collaboration, T. Coan et al., *Measurement of* α_s *from tau decays*, *Phys. Lett.* **B356** (1995) 580–588.

[31] **OPAL** Collaboration, K. Ackerstaff et al., *Measurement of the strong coupling constant* α_s *and the vector and axial vector spectral functions in hadronic tau decays*, *Eur. Phys. J.* **C7** (1999) 571–593, [hep-ex/9808019].

[32] A. Pich, *Precision Tau Physics*, *Prog. Part. Nucl. Phys.* **75** (2014) 41–85, [arXiv:1310.7922].

[33] D. Boito, M. Golterman, K. Maltman, J. Osborne, and S. Peris, *Strong coupling from the revised ALEPH data for hadronic τ decays*, *Phys. Rev.* **D91** (2015), no. 3 034003, [arXiv:1410.3528].

[34] D. Boito, M. Golterman, K. Maltman, and S. Peris, *Strong coupling from hadronic τ decays: A critical appraisal*, *Phys. Rev.* **D95** (2017), no. 3 034024, [arXiv:1611.03457].

[35] D. Boito, M. Golterman, K. Maltman, and S. Peris, *Determining* α_s *from hadronic τ decay: the pitfalls of truncating the OPE*, in *15th International Workshop on Tau Lepton Physics (TAU2018) Amsterdam, Netherlands, September 24-28, 2018*, 2018. arXiv:1811.01581.

[36] A. Pich and A. Rodríguez-Sánchez, *Updated determination of* $\alpha_s(m_\tau^2)$ *from tau decays*, *Mod. Phys. Lett.* **A31** (2016), no. 30 1630032, [arXiv:1606.07764].

[37] A. Pich, *Tau-decay determination of the strong coupling*, in *15th International Workshop on Tau Lepton Physics (TAU2018) Amsterdam, Netherlands, September 24-28, 2018*, 2018. arXiv:1811.10067.

[38] A. Pich and A. Rodríguez-Sánchez, *Determination of the QCD coupling from ALEPH τ decay data*, *Phys. Rev.* **D94** (2016), no. 3 034027, [arXiv:1605.06830].

[39] S. I. Eidelman, L. M. Kurdadze, and A. I. Vainshtein, *e^+e^- Annihilation Into Hadrons Below 2 GeV. Test of QCD Predictions*, *Phys. Lett.* **82B** (1979) 278–280.

[40] S. Narison and A. Pich, *Semiinclusive tau decays involving the vector or axial-vector hadronic currents*, *Phys. Lett.* **B304** (1993) 359–365.

[41] D. Boito, M. Golterman, A. Keshavarzi, K. Maltman, D. Nomura, S. Peris, and T. Teubner, *Strong coupling from $e^+e^- \to$ hadrons below charm*, *Phys. Rev.* **D98** (2018), no. 7 074030, [arXiv:1805.08176].

[42] J. Gao, L. Harland-Lang, and J. Rojo, *The Structure of the Proton in the LHC Precision Era*, *Phys. Rept.* **742** (2018) 1–121, [arXiv:1709.04922].

[43] A. Accardi et al., *A Critical Appraisal and Evaluation of Modern PDFs*, *Eur. Phys. J.* **C76** (2016), no. 8 471, [arXiv:1603.08906].

[44] J. Rojo et al., *The PDF4LHC report on PDFs and LHC data: Results from Run I and preparation for Run II*, *J. Phys.* **G42** (2015) 103103, [arXiv:1507.00556].

[45] J. Rojo, *Constraints on parton distributions and the strong coupling from LHC jet data*, *Int. J. Mod. Phys.* **A30** (2015) 1546005, [arXiv:1410.7728].

[46] J. M. Campbell, J. Rojo, E. Slade, and C. Williams, *Direct photon production and PDF fits reloaded*, *Eur. Phys. J.* **C78** (2018), no. 6 470, [arXiv:1802.03021].

[47] R. Boughezal, A. Guffanti, F. Petriello, and M. Ubiali, *The impact of the LHC Z-boson transverse momentum data on PDF determinations*, *JHEP* **07** (2017) 130, [arXiv:1705.00343].

[48] M. Czakon, N. P. Hartland, A. Mitov, E. R. Nocera, and J. Rojo, *Pinning down the large-x gluon with NNLO top-quark pair differential distributions*, *JHEP* **04** (2017) 044, [arXiv:1611.08609].

[49] **NNPDF** Collaboration, R. D. Ball, S. Carrazza, L. Del Debbio, S. Forte, Z. Kassabov, J. Rojo, E. Slade, and M. Ubiali, *Precision determination of the strong coupling constant within a global PDF analysis*, *Eur. Phys. J.* **C78** (2018), no. 5 408, [arXiv:1802.03398].

[50] **NNPDF** Collaboration, R. D. Ball et al., *Parton distributions from high-precision collider data*, *Eur. Phys. J.* **C77** (2017), no. 10 663, [arXiv:1706.00428].

[51] S. Lionetti et al., *Precision determination of α_s using an unbiased global NLO parton set*, *Phys. Lett.* **B701** (2011) 346–352, [arXiv:1103.2369].

[52] R. D. Ball, V. Bertone, L. Del Debbio, S. Forte, A. Guffanti, et al., *Precision NNLO determination of $\alpha_s(M_Z)$ using an unbiased global parton set*, *Phys.Lett.* **B707** (2012) 66–71, [arXiv:1110.2483].

[53] L. A. Harland-Lang, A. D. Martin, P. Motylinski, and R. S. Thorne, *Uncertainties on α_S in the MMHT2014 global PDF analysis and implications for SM predictions*, *Eur. Phys. J.* **C75** (2015), no. 9 435, [arXiv:1506.05682].

[54] S. Alekhin, J. Blümlein, S. Moch, and R. Placakyte, *Parton distribution functions, α_s, and heavy-quark masses for LHC Run II*, *Phys. Rev.* **D96** (2017), no. 1 014011, [arXiv:1701.05838].

[55] R. Thorne, *The effect on PDFs and $\alpha_S(M_Z^2)$ due to changes in flavour scheme and higher twist contributions*, *Eur.Phys.J.* **C74** (2014), no. 7 2958, [arXiv:1402.3536].

[56] S. Alekhin, J. Blumlein, and S. Moch, *Parton Distribution Functions and Benchmark Cross Sections at NNLO*, *Phys. Rev.* **D86** (2012) 054009, [arXiv:1202.2281].

[57] J. Currie, E. W. N. Glover, and J. Pires, *Next-to-Next-to Leading Order QCD Predictions for Single Jet Inclusive Production at the LHC*, *Phys. Rev. Lett.* **118** (2017), no. 7 072002, [arXiv:1611.01460].

[58] J. Currie, A. Gehrmann-De Ridder, T. Gehrmann, E. W. N. Glover, A. Huss, and J. Pires, *Precise predictions for dijet production at the LHC*, *Phys. Rev. Lett.* **119** (2017), no. 15 152001, [arXiv:1705.10271].

[59] M. Czakon, D. Heymes, and A. Mitov, *Dynamical scales for multi-TeV top-pair production at the LHC*, *JHEP* **04** (2017) 071, [arXiv:1606.03350].

[60] **H1** Collaboration, V. Andreev et al., *Determination of the strong coupling constant $\alpha_s(m_Z)$ in next-to-next-to-leading order QCD using H1 jet cross section measurements*, *Eur. Phys. J.* **C77** (2017), no. 11 791, [arXiv:1709.07251].

[61] J. Currie, T. Gehrmann, A. Huss, and J. Niehues, *NNLO QCD corrections to jet production in deep inelastic scattering*, *JHEP* **07** (2017) 018, [arXiv:1703.05977].

[62] S. Alekhin et al., *HERAFitter*, *Eur. Phys. J.* **C75** (2015), no. 7 304, [arXiv:1410.4412].

[63] T. Klijnsma, S. Bethke, G. Dissertori, and G. P. Salam, *Determination of the strong coupling constant $\alpha_s(m_Z)$ from measurements of the total cross section for top-antitop quark production*, *Eur. Phys. J.* **C77** (2017), no. 11 778, [arXiv:1708.07495].

[64] **CMS** Collaboration, S. Chatrchyan et al., *Determination of the top-quark pole mass and strong coupling constant from the t t-bar production cross section in pp collisions at $\sqrt{s}$ = 7 TeV*, *Phys.Lett.* **B728** (2014) 496, [arXiv:1307.1907].

[65] **NNPDF** Collaboration, R. D. Ball et al., *Parton distributions for the LHC Run II*, *JHEP* **04** (2015) 040, [arXiv:1410.8849].

[66] **CMS** Collaboration, S. Chatrchyan et al., *Measurement of the ratio of the inclusive 3-jet cross section to the inclusive 2-jet cross section in pp collisions at $\sqrt{s}$ = 7 TeV and first determination of the strong coupling constant in the TeV range*, *Eur. Phys. J.* **C73** (2013), no. 10 2604, [arXiv:1304.7498].

[67] **CMS** Collaboration, V. Khachatryan et al., *Constraints on parton distribution functions and extraction of the strong coupling constant from the inclusive jet cross section in pp collisions at $\sqrt{s}$ = 7 TeV*, *Eur. Phys. J.* **C75** (2015), no. 6 288, [arXiv:1410.6765].

[68] **ATLAS** Collaboration, M. Aaboud et al., *Determination of the strong coupling constant α_s from transverse energy–energy correlations in multijet events at $\sqrt{s}$ = 8 TeV using the ATLAS detector*, *Eur. Phys. J.* **C77** (2017), no. 12 872, [arXiv:1707.02562].

[69] **ATLAS** Collaboration, M. Aaboud et al., *Measurement of dijet azimuthal decorrelations in pp collisions at $\sqrt{s}$ = 8 TeV with the ATLAS detector and determination of the strong coupling*, arXiv:1805.04691.

[70] S. Dimopoulos, S. Raby, and F. Wilczek, *Supersymmetry and the Scale of Unification*, *Phys. Rev.* **D24** (1981) 1681–1683.

[71] D. Becciolini, M. Gillioz, M. Nardecchia, F. Sannino, and M. Spannowsky, *Constraining new colored matter from the ratio of 3 to 2 jets cross sections at the LHC*, *Phys. Rev.* **D91** (2015), no. 1 015010, [arXiv:1403.7411]. [Addendum: Phys. Rev.D92,no.7,079905(2015)].

PoS(Confinement2018)035

[72] **CMS** Collaboration, *Determination of the strong coupling constant from the measurement of inclusive multijet event cross sections in pp collisions at* $\sqrt{s} = 8$ TeV, Tech. Rep. CMS-PAS-SMP-16-008, CERN, Geneva, 2017.

[73] A. H. Hoang, D. W. Kolodrubetz, V. Mateu, and I. W. Stewart, *Precise determination of* α_s *from the C-parameter distribution*, *Phys. Rev.* **D91** (2015), no. 9 094018, [arXiv:1501.04111].

[74] R. Abbate, M. Fickinger, A. H. Hoang, V. Mateu, and I. W. Stewart, *Thrust at* N^3LL *with Power Corrections and a Precision Global Fit for alphas(mZ)*, *Phys. Rev.* **D83** (2011) 074021, [arXiv:1006.3080].

[75] S. Aoki et al., *Review of lattice results concerning low-energy particle physics*, *Eur. Phys. J.* **C77** (2017), no. 2 112, [arXiv:1607.00299].

[76] K. G. Wilson, *Confinement of Quarks*, *Phys. Rev.* **D10** (1974) 2445–2459. [,319(1974)].

[77] L. Susskind, *Coarse Grained Quantum Chromodynamics*, in *Ecole d'Ete de Physique Theorique - Weak and Electromagnetic Interactions at High Energy Les Houches, France, July 5-August 14, 1976*, pp. 207–308, 1976.

[78] W. Fischler, *Quark - anti-Quark Potential in QCD*, *Nucl. Phys.* **B129** (1977) 157–174.

[79] L. S. Brown and W. I. Weisberger, *Remarks on the Static Potential in Quantum Chromodynamics*, *Phys. Rev.* **D20** (1979) 3239.

[80] N. Brambilla, A. Pineda, J. Soto, and A. Vairo, *The Infrared behavior of the static potential in perturbative QCD*, *Phys. Rev.* **D60** (1999) 091502, [hep-ph/9903355].

[81] N. Brambilla, A. Pineda, J. Soto, and A. Vairo, *Potential NRQCD: An Effective theory for heavy quarkonium*, *Nucl. Phys.* **B566** (2000) 275, [hep-ph/9907240].

[82] C. Anzai, Y. Kiyo, and Y. Sumino, *Static QCD potential at three-loop order*, *Phys. Rev. Lett.* **104** (2010) 112003, [arXiv:0911.4335].

[83] A. V. Smirnov, V. A. Smirnov, and M. Steinhauser, *Three-loop static potential*, *Phys. Rev. Lett.* **104** (2010) 112002, [arXiv:0911.4742].

[84] N. Brambilla, X. Garcia i Tormo, J. Soto, and A. Vairo, *The Logarithmic contribution to the QCD static energy at* N^4LO, *Phys. Lett.* **B647** (2007) 185–193, [hep-ph/0610143].

[85] A. Pineda and J. Soto, *The Renormalization group improvement of the QCD static potentials*, *Phys. Lett.* **B495** (2000) 323–328, [hep-ph/0007197].

[86] N. Brambilla, A. Vairo, X. Garcia i Tormo, and J. Soto, *The QCD static energy at NNNLL*, *Phys. Rev.* **D80** (2009) 034016, [arXiv:0906.1390].

[87] X. Garcia i Tormo, *Review on the determination of* α_s *from the QCD static energy*, *Mod. Phys. Lett.* **A28** (2013) 1330028, [arXiv:1307.2238].

[88] A. Pineda, *Heavy quarkonium and nonrelativistic effective field theories*, Ph.D. Thesis, University of Barcelona (1998) (1998). (Ph.D. Thesis, University of Barcelona).

[89] A. H. Hoang, M. C. Smith, T. Stelzer, and S. Willenbrock, *Quarkonia and the pole mass*, *Phys. Rev.* **D59** (1999) 114014, [hep-ph/9804227].

[90] S. Necco and R. Sommer, *Testing perturbation theory on the N(f) = 0 static quark potential*, *Phys. Lett.* **B523** (2001) 135–142, [hep-ph/0109093].

29

[91] N. Brambilla, X. Garcia i Tormo, J. Soto, and A. Vairo, *Precision determination of $r_0\Lambda_{\overline{MS}}$ from the QCD static energy*, *Phys. Rev. Lett.* **105** (2010) 212001, [`arXiv:1006.2066`]. [Erratum: Phys. Rev. Lett.108,269903(2012)].

[92] N. Husung, M. Koren, P. Krah, and R. Sommer, *SU(3) Yang Mills theory at small distances and fine lattices*, *EPJ Web Conf.* **175** (2018) 14024, [`arXiv:1711.01860`].

[93] **ETM** Collaboration, K. Jansen, F. Karbstein, A. Nagy, and M. Wagner, $\Lambda_{\overline{MS}}$ *from the static potential for QCD with $n_f = 2$ dynamical quark flavors*, *JHEP* **01** (2012) 025, [`arXiv:1110.6859`].

[94] F. Karbstein, A. Peters, and M. Wagner, $\Lambda_{\overline{MS}}^{(n_f=2)}$ *from a momentum space analysis of the quark-antiquark static potential*, *JHEP* **09** (2014) 114, [`arXiv:1407.7503`].

[95] F. Karbstein, M. Wagner, and M. Weber, *Determination of* $\Lambda_{\overline{MS}}^{(n_f=2)}$ *and analytic parameterization of the static quark-antiquark potential*, `arXiv:1804.10909`.

[96] A. Bazavov, N. Brambilla, X. Garcia i Tormo, P. Petreczky, J. Soto, and A. Vairo, *Determination of α_s from the QCD static energy*, *Phys. Rev.* **D86** (2012) 114031, [`arXiv:1205.6155`].

[97] A. Bazavov, N. Brambilla, X. Garcia i Tormo, P. Petreczky, J. Soto, and A. Vairo, *Determination of α_s from the QCD static energy: An update*, *Phys. Rev.* **D90** (2014), no. 7 074038, [`arXiv:1407.8437`].

[98] A. Vairo, *Strong coupling from the QCD static energy*, *Mod. Phys. Lett.* **A31** (2016), no. 34 1630039.

[99] H. Takaura, T. Kaneko, Y. Kiyo, and Y. Sumino, *Determination of α_s from static QCD potential with renormalon subtraction*, `arXiv:1808.01632`.

[100] H. Takaura, T. Kaneko, Y. Kiyo, and Y. Sumino, *Determination of α_s from static QCD potential: OPE with renormalon subtraction and Lattice QCD*, `arXiv:1808.01643`.

[101] **MILC** Collaboration, A. Bazavov et al., *Results for light pseudoscalar mesons*, *PoS* **LATTICE2010** (2010) 074, [`arXiv:1012.0868`].

[102] S. Necco and R. Sommer, *The N(f) = 0 heavy quark potential from short to intermediate distances*, *Nucl. Phys.* **B622** (2002) 328–346, [`hep-lat/0108008`].

[103] A. Bazavov, N. Brambilla, X. Garcia i Tormo, P. Petreczky, J. Soto, A. Vairo, and J. Weber *TUM-EFT 111/18 (2018)* (2018).

[104] A. Bazavov, P. Petreczky, and J. H. Weber, *Equation of State in 2+1 Flavor QCD at High Temperatures*, *Phys. Rev.* **D97** (2018), no. 1 014510, [`arXiv:1710.05024`].

[105] D. Eiras and J. Soto, *Light fermion finite mass effects in non-relativistic bound states*, *Phys. Lett.* **B491** (2000) 101–110, [`hep-ph/0005066`].

[106] N. Brambilla, A. Pineda, J. Soto, and A. Vairo, *The QCD potential at O(1/m)*, *Phys. Rev.* **D63** (2001) 014023, [`hep-ph/0002250`].

[107] Y. Koma, M. Koma, and H. Wittig, *Nonperturbative determination of the QCD potential at O(1/m)*, *Phys. Rev. Lett.* **97** (2006) 122003, [`hep-lat/0607009`].

[108] R. Sommer, *Scale setting in lattice QCD*, *PoS* **LATTICE2013** (2014) 015.

[109] W. Bernreuther and W. Wetzel, *Decoupling of heavy quarks in the minimal subtraction scheme*, *Nucl.Phys.* **B197** (1982) 228.

[110] B. A. Kniehl, A. V. Kotikov, A. I. Onishchenko, and O. L. Veretin, *Strong-coupling constant with flavor thresholds at five loops in the anti-MS scheme*, *Phys. Rev. Lett.* **97** (2006) 042001.

PoS(Confinement2018)035

[111] T. van Ritbergen, J. A. M. Vermaseren, and S. A. Larin, *The four-loop β-function in quantum chromodynamics*, *Phys. Lett.* **B400** (1997) 379–384, [hep-ph/9701390].

[112] M. Czakon, *The Four-loop QCD beta-function and anomalous dimensions*, *Nucl. Phys.* **B710** (2005) 485–498.

[113] A. G. Grozin, M. Hoeschele, J. Hoff, and M. Steinhauser, *Simultaneous decoupling of bottom and charm quarks*, *JHEP* **09** (2011) 066.

[114] A. Athenodorou, J. Finkenrath, F. Knechtli, T. Korzec, B. Leder, M. Marinkovic, and R. Sommer, *How perturbative are heavy sea quarks?*, arXiv:1809.03383.

[115] K. Symanzik. In: Recent Developments in Gauge Theories, edited by G. 't Hooft et al. (Plenum Press, New York, 1980), p. 313.

[116] G. P. Lepage and P. B. Mackenzie, *On the viability of lattice perturbation theory*, *Phys. Rev.* **D48** (1993) 2250–2264.

[117] M. Lüscher, P. Weisz, and U. Wolff, *A numerical method to compute the running coupling in asymptotically free theories*, *Nucl.Phys.* **B359** (1991) 221–243.

[118] **ALPHA** Collaboration, M. Dalla Brida, P. Fritzsch, T. Korzec, A. Ramos, S. Sint, and R. Sommer, *A non-perturbative exploration of the high energy regime in $N_\mathrm{f} = 3$ QCD*, *Eur. Phys. J.* **C78** (2018), no. 5 372, [arXiv:1803.10230].

[119] S. Aoki et al., *Review of lattice results concerning low-energy particle physics*, *Eur. Phys. J.* **C74** (2014) 2890, [arXiv:1310.8555].

[120] R. Hudspith, R. Lewis, K. Maltman, and E. Shintani, *α_s from the Hadronic Vacuum Polarisation*, *EPJ Web Conf.* **175** (2018) 10006.

[121] K. Nakayama, H. Fukaya, and S. Hashimoto, *Lattice computation of the Dirac eigenvalue density in the perturbative regime of QCD*, *Phys. Rev.* **D98** (2018), no. 1 014501.

[122] [ALPHA 16] M. Dalla Brida, P. Fritzsch, T. Korzec, A. Ramos, S. Sint, and R. Sommer, *Determination of the QCD Λ-parameter and the accuracy of perturbation theory at high energies*, *Phys. Rev. Lett.* **117** (2016), no. 18 182001.

[123] [ALPHA 17] M. Bruno, M. Dalla Brida, P. Fritzsch, T. Korzec, A. Ramos, S. Schaefer, H. Simma, S. Sint, and R. Sommer, *QCD Coupling from a Nonperturbative Determination of the Three-Flavor Λ Parameter*, *Phys. Rev. Lett.* **119** (2017), no. 10 102001.

[124] [PACS-CS 09A] S. Aoki et al., *Precise determination of the strong coupling constant in $N_f = 2 + 1$ lattice QCD with the Schrödinger functional scheme*, *JHEP* **0910** (2009) 053.

[125] R. J. Hudspith, R. Lewis, K. Maltman, and E. Shintani, *α_s from the Lattice Hadronic Vacuum Polarisation*, arXiv:1804.10286.

[126] [JLQCD 10] E. Shintani, S. Aoki, H. Fukaya, S. Hashimoto, T. Kaneko, et al., *Strong coupling constant from vacuum polarization functions in three-flavor lattice QCD with dynamical overlap fermions*, *Phys.Rev.* **D82** (2010) 074505, Erratum–ibid. **D89** (2014) 099903.

[127] [HPQCD 10] C. McNeile, C. T. H. Davies, E. Follana, K. Hornbostel and G. P. Lepage, *High-precision c and b masses and QCD coupling from current-current correlators in lattice and continuum QCD*, *Phys. Rev.* **D82** (2010) 034512.

[128] K. Maltman, D. Leinweber, P. Moran, and A. Sternbeck, *The realistic lattice determination of $\alpha_s(M_Z)$ revisited*, *Phys. Rev.* **D78** (2008) 114504.

[129] [JLQCD 16] K. Nakayama, B. Fahy, and S. Hashimoto, *Short-distance charmonium correlator on the lattice with Möbius domain-wall fermion and a determination of charm quark mass*, *Phys. Rev.* **D94** (2016), no. 5 054507.

[130] Y. Maezawa and P. Petreczky, *Quark masses and strong coupling constant in 2+1 flavor QCD*, *Phys. Rev.* **D94** (2016), no. 3 034507.

[131] [HPQCD 14A] B. Chakraborty, C. T. H. Davies, G. C. Donald, R. J. Dowdall, B. Galloway, P. Knecht, J. Koponen, G. P. Lepage, and C. McNeile, *High-precision quark masses and QCD coupling from $n_f = 4$ lattice QCD*, *Phys.Rev.* **D91** (2015) 054508.

[132] [HPQCD 08B] I. Allison et al., *High-precision charm-quark mass from current-current correlators in lattice and continuum QCD*, *Phys. Rev.* **D78** (2008) 054513.

[133] [ETM 13D] B. Blossier et al., *High statistics determination of the strong coupling constant in Taylor scheme and its OPE Wilson coefficient from lattice QCD with a dynamical charm*, *Phys.Rev.* **D89** (2014) 014507.

[134] [ETM 12C] B. Blossier, P. Boucaud, M. Brinet, F. De Soto, X. Du, et al., *The strong running coupling at τ and Z_0 mass scales from lattice QCD*, *Phys.Rev.Lett.* **108** (2012) 262002.

[135] [ETM 11D] B. Blossier, P. Boucaud, M. Brinet, F. De Soto, X. Du, et al., *Ghost-gluon coupling, power corrections and $\Lambda_{\overline{MS}}$ from lattice QCD with a dynamical charm*, *Phys.Rev.* **D85** (2012) 034503.

[136] C. Patrignani et al., *Review of Particle Physics*, *Chin. Phys.* **C40** (2016), no. 10 100001.